Novel derivatives of BCV and (S)-HPMPA inhibit orthopoxviruses and human adenoviruses more potently than BCV

Yifan Zhang[1,2,§], Yanmin Wan[1,3,#,§], Cuiyuan Guo[2,4,§], Zhaoqin Zhu[2,5,§], Chao Qiu[6,§], Jiasheng Lu[7,8,9], Yanan Zhou[10], Jiaojiao Zheng[5], Fahui Dai[5], Xiaoyang Cheng[1,2], Kunlu Deng[1,2], Wanhai Wang[3], Youchun Wang[10,11,#], Wenhong Zhang[1, #]

[1] Department of Infectious Diseases, Shanghai Key Laboratory of Infectious Diseases and Biosafety Emergency Response, National Medical Center for Infectious Diseases, Huashan Hospital, State Key Laboratory of Genetic Engineering, School of Life Science, Fudan University, China; Shanghai Sci-Tech Inno Center for Infection & Immunity, Shanghai 200052, China

[2] Department of laboratory medicine, Shanghai Public Health Clinical Center, Shanghai 201508, China

[3] Department of radiology, Shanghai Public Health Clinical Center, Shanghai 201508, China

[4] Clinical Laboratory, The First Affiliated Hospital of Zhengzhou University, Key Laboratory of Laboratory Medicine of Henan Province, Zhengzhou 450052, China

[5] Biosafety Level 3 Laboratory, Shanghai Public Health Clinical Center, Shanghai 201508, China

[6] Institutes of biomedical sciences & Shanghai Key Laboratory of Medical Epigenetics, Fudan University, Shanghai, China

[7] School of Life Sciences, Fudan University, Shanghai 200437, China

[8] Shenzhen Institutes of Advanced Technology, Chinese Academy of Sciences, Shenzhen 518055, China

[9] Risen (Shanghai) Pharma Tech Co., Ltd., Shanghai 201210, China

[10] Institute of Medical Biology, Chinese Academy of Medical Sciences and Peking Union Medical College, Kunming, China

[11] Key Laboratory of Pathogen Infection Prevention and Control (Peking Union Medical College), Ministry of Education, Beijing, China; State Key Laboratory of Respiratory Health and Multimorbidity, Beijing, China

[§] These authors contribute equally: Yifan Zhang, Yanmin Wan, Cuiyuan Guo, Zhaoqin Zhu and Chao Qiu

[#] These authors jointly supervised this work: Yanmin Wan, yanmin_wan@fudan.edu.cn; Youchun Wang, wangyc@nifdc.org.cn; Wenhong Zhang, zhangwenhong@fudan.edu.cn;

Running title: Novel prodrugs inhibit orthopoxviruses more potently than BCV

Word counts: main text, 4480 words; abstract, 240 words.

Abstract

BCV and tecovirimat are the only two chemical drugs that have been approved to treat smallpox and can be requested for Mpox treatment through a single-patient Emergency Investigational New Drug (EIND) application. Disappointedly, the efficacy of tecovirimat manifested in a recent clinical trial is far from being satisfactory, while the clinical efficacy of BCV is still inconclusive. Given that MPXV, variola and other emerging orthopoxviruses are posing serious threats to global health, it is urgent to develop better therapeutics. In this study, we tested the antiviral effects of three novel prodrugs, which were designed based on previously reported parent drugs, either (S)-HPMPC (cidofovir) or (S)-HPMPA. We found that one of the (S)-HPMPA-based prodrugs, ODE-(S)-HPMPA formate, exhibited significantly better anti-orthopoxvirus activity than BCV both in vitro and in vivo, which also inhibited human adenovirus type 2 and type 21 more efficiently than BCV. Most strikingly, the EC_{50} and EC_{90} of ODE-(S)-HPMPA formate against MPXV were more than 40-fold lower than those of BCV. In contrast, we observed that the anti-HSV-1 activities of the (S)-HPMPA-based prodrugs were less effective than those of the cidofovir-based prodrugs (BCV and BCV formate), especially in vivo. Moreover, we showed for the first time that cytidine and adenine analog combined therapies could provide mice with complete protection against lethal challenges of both vaccinia and HSV-1. Collectively, we propose that both the ODE-(S)-HPMPA formate and the BCV/ODE-(S)-HPMPA formate combination are worth further investigations for their potential clinical applications.

Key words: Orthopoxvirus, HSV, Human adenovirus, Nucleos(t)ide analogue, BCV

Introduction

Viral polymerases are the most sought-after targets for developing anti-viral drugs [1-3]. Few dozens of viral RNA or DNA dependent polymerase inhibitors have been licensed for the treatment of human viral diseases, including brincidofovir (BCV, a prodrug of cidofovir), which is the second FDA approved drug for the treatment of smallpox infection [3, 4]. Given that variola and monkeypox virus (MPXV) are phylogenetically similar, the U.S. CDC suggests that BCV can be requested for the treatment of human Mpox disease in adults and pediatric patients through a single-patient Emergency Investigational New Drug (EIND) application.

BCV is a lipid conjugate of the nucleotide analogue cidofovir with broad-spectrum anti-double stranded DNA virus activity [5]. Data of previous studies suggested that the in vitro 50% inhibitory concentration (IC_{50}) of BCV against MPXV was relatively higher than that of tecovirimat [6-8], a specific inhibitor of orthopoxviruses targeting viral p37 protein orthologs [9]. Both compounds have been used to treat human Mpox disease [8, 10], but BCV can elevate the transaminases in the liver [11-13]. Tecovirimat has a relatively better safety profile [14] and is currently recommended by the U.S. CDC to be the first line treatment for MPXV infections in people. But at the same time, the U.S. CDC also alerts in the Guidance for Tecovirimat Use (https://www.cdc.gov/poxvirus/mpox/clinicians/Tecovirimat.html) that tecovirimat has a low barrier to viral resistance. A single amino acid mutation to the orthopoxviral p37 protein can lead to resistance to tecovirimat [15], which may be especially prong to occurrence among severely immunocompromised Mpox patients under multiple courses of tecovirimat treatment [16, 17]. Besides, according to data released from a clinical trial in the Democratic Republic of the Congo, tecovirimat neither accelerated recovery nor reduced mortality rate compared to placebo [18].

Mutations associated with cidofovir resistance have also been identified in multiple orthopoxviruses [8, 19] and human cytomegalovirus [20]. And mutations potentially associated with CDV resistance among the MPXVs of 2022 outbreak have been reported, too [8]. The prevalence of mutated MPXV may further rise once BCV was more widely and frequently used, which is also true for other orthopoxviruses because the mechanism of CDV resistance seems to be shared among the genus [21]. Given the

108 pacing threats posed by MPXV, variola and other emerging orthopoxviruses to human
109 health [22-25] , it is urgent to develop safer and more effective drugs.
110 CDV [(S)-1-(3-hydroxy-2-phosphonylmethoxypropyl)cytosine, HPMPC] and its prodrug
111 BCV exemplify that the (S)-HPMP nucleoside can be a promising class of broad
112 spectrum anti-viral compounds [5]. In fact, many others candidate molecules in this
113 class have been synthesized and tested for anti-viral effects. (S)-HPMPA [(S)-9-(3-
114 hydroxy-2-phosphonomethoxypropyl)-adenine] is one of these candidates, which
115 showed broad spectrum anti-viral activities in earlier studies [5, 26]. However, because
116 of the poor oral bioavailability, (S)-HPMPA is considered as not suitable for clinical use.
117 Great efforts have been made to modify (S)-HPMPA in order to increase their oral
118 bioavailabilities and anti-viral activities [27-35]. But only few candidate compounds, such
119 as ODE-(S)-HPMPA and HDP-(S)-HPMPA, displayed promising in vivo anti-
120 orthopoxvirus effects [30, 33]. In this work, we synthesized two novel (S)-HPMPA
121 prodrugs, ODE-(S)-HPMPA formate and HDP-(S)-HPMPA formate, and a new CDV
122 prodrug, BCV formate, and tested their anti-viral effects in parallel with BCV both in vitro
123 and in vivo.
124
125 **Materials and methods**
126 **Ethical Statement**
127 Experiments using mice were approved by the Research Ethics Review Committee of
128 the Shanghai Public Health Clinical Center Affiliated to Fudan University. Experiments
129 using live vaccinia, HSV-1 and adenoviruses were conducted in a BSL-2 or ABSL-2 lab.
130 Measurements of in vitro inhibition of MPXV were performed in a BSL-3 lab.
131 **Antiviral compounds**
132 BCV (CAS number 444805-28-1, purity 99.82%) was purchased from Shanghai
133 Haohong Scientific Co., Ltd.. Three candidate compounds were synthesized by our
134 collaborator, Risen (Shanghai) Pharma Tech Co., Ltd. Compound BCV formate (purity
135 97.86%) is a derivative of cidofovir. Compound ODE-(S)-HPMPA formate (purity
136 95.03%) and compound HDP-(S)-HPMPA formate (purity 96.97%) are prodrugs of (S)-
137 HPMPA. The molecular formulas of these compounds and their active metabolites are
138 shown in Figure1.

139 **Virus propagation and titration**

140 Vaccinia Tiantan strain was propagated in Vero cells. Briefly, confluent Vero cells plated
141 in 100mm×10mm petri dishes were inoculated with Tiantan vaccinia at a multiplicity of
142 infection (MOI) of 0.01. After 2 hours absorption at 37°C with 5% CO_2, the inoculum was
143 removed and 10ml of fresh maintenance medium (DMEM containing 3% FBS and 1%
144 PS) was added to each dish. The cell cultures were maintained at 37°C with 5% CO_2 for
145 another 2 days. After that, propagated vaccinia viruses were harvested by three rapid
146 freeze-thaw cycles of the infected cells. HSV-1 propagation followed a similar protocol
147 except that the inoculum was adsorbed for 1 hour with gentle agitation at room
148 temperature and the propagated virus was harvested from the culture supernatant by
149 centrifuging at 34,000g for 2 hours at 4°C [36]. MPXV was sourced from National
150 Kunming High-level Biosafety Primate Research Center, Institute of Medical Biology,
151 Chinese Academy of Medical Sciences and Peking Union Medical College. Viruses
152 were amplified in Vero cells, cultured in DMEM supplemented with 2% FBS and 1% PS.
153 Harvested vaccinia, MPXV and HSV-1 viruses were titrated using plaque assays. Briefly,
154 confluent monolayers of Vero cells in 24-well plates were infected with 10-fold serial
155 dilutions of each virus, ranging from 10^{-1} to 10^{-9}. For vaccinia viruses and MPXV, the
156 plates were incubated at 37°C with 5% CO_2 for 2 hours. For HSV-1 (strain-17), the
157 plates were gently agitated at room temperature for 1 hour. After absorption, the cells
158 were overlaid with 800 μL of overlay medium (DMEM containing 1% FBS and 1.25%
159 methyl cellulose) and incubated at 37°C with 5% CO_2 for 4 days. Post-incubation, the
160 plates were fixed with 4% neutral formalin and stained with crystal violet. Plaques were
161 visually counted, and the viral titers were calculated and expressed as plaque-forming
162 units (PFU) per milliliter.

163 HAdV-B21 and C2 were isolated from nasopharyngeal swab specimens of HAdV-
164 positive patients and propagated in HEp-2 cells. Briefly, HEp-2 cells were plated in
165 100mm×10mm petri dishes and inoculated with hAdVs. After a 1-hour adsorption at 37°
166 C with 5% CO_2, the inoculum was removed, and 10 mL of maintenance medium was
167 added to each dish. The cultures were maintained at 37°C with 5% CO_2 until more than
168 80% of the cells exhibited cytopathic effects (CPE). Propagated hAdVs were harvested
169 by three rapid freeze-thaw cycles of the infected cells.

170 The stocks of hAdVs were titrated using the $TCID_{50}$ assay. Briefly, confluent monolayers
171 of Vero cells in 96-well cell culture plates were infected with 10-fold serial dilutions of
172 the hAdVs. The wells were monitored for the presence of CPE and the infectious
173 adenovirus titer was determined as $TCID_{50}$ per mL using the Spearman-Karber method.

174 **Cytotoxicity assays**

175 The cytotoxicities of candidate compounds were determined using a Promega CellTiter-
176 Glo® Luminescent Cell Viability Assay kit (Cat#G7571, Madison, WI, USA) according to
177 the manufacturer's instructions. Briefly, Vero cells were seeded in 96-well plates and
178 incubated overnight. Then, cells were exposed to either the solvent control (DCM:MeOH,
179 v:v=1:3) or diluted candidate compounds. Each concentration was tested in
180 quadruplicate. The plates were incubated for 72 hours at 37°C with 5% CO_2.
181 Subsequently, reconstituted Steady-Glo reagent was added and assay plates were
182 incubated for 10 min at room temperature. The luminescence was measured using a
183 luminescence microplate reader (GloMax® Navigator Microplate Luminometer,
184 Promega, USA). Wells containing culture medium without cells served as blank controls.
185 Cell viabilities were calculated using the following equation: Cell viability (%) = (drug
186 treated well - blank) / (solvent treated well - blank) × 100%.

187 **In vitro viral inhibition assays**

188 Twenty PFU of orthopoxvirus (Tiantan vaccinia or MPXV) or HSV-1 virus suspended in
189 200 μL maintenance medium were transferred onto confluent Vero cell monolayers in
190 24-well plates. For vaccinia virus, the plates were incubated at 37°C with 5% CO_2 for 2
191 hours. For HSV-1, the plates were gently agitated at room temperature for 1 hour. 800
192 μL of overlay-medium containing DCM:MeOH (v:v=1:3) or serially diluted candidate
193 compounds was added to each well after removing the inoculums. The plates were then
194 incubated for 4 days at 37°C with 5% CO_2. Finally, the plates were fixed with 4% neutral
195 formalin and stained with crystal violet. The number of plaques in each well was visually
196 counted. All compounds were tested in quadruplicates at each dilution. The viral
197 inhibition rate was calculated using the formula: Inhibition rate (%) = (1 − the average
198 plaque number of the sample wells / the average plaque number of the solvent wells) ×
199 100%.

200 In vitro inhibition of hAdV B21 and C2 were performed as described previously [37].
201 Briefly, 25,000 Vero cells were plated in each well of a 96-well cell culture plate,
202 followed by addition of diluted adenovirus (with 50 and 200 $TCID_{50}$/well for B21 and C2,
203 respectively) and serially diluted candidate compounds. The solvent was used as the
204 non-treated control. The plates were then incubated at 37°C with 5% CO_2 for 4 days.
205 Cytopathology was quantitively assessed using a Promega CellTiter-Glo® Luminescent
206 Cell Viability Assay kit. The viral inhibition rate was calculated using the formula:
207 inhibition rate (%) = (drug treated well – blank) - (non-treated control well – blank) ×
208 100%.

209 **In vivo evaluation of anti-viral effects**

210 We established mouse infection models to evaluate the anti-viral effects of the
211 candidate compounds against Tiantan vaccinia and HSV-1, respectively. Vaccinia
212 Tiantan strain (6×10^6 PFU) was suspended in 40 μL 1×PBS and instilled intranasally
213 into 4-week-old male BALB/c mice under transient anesthesia of inhaled isoflurane
214 (Cat# R510-22, Ryward RWD). For HSV-1 infections, 4-week-old female BALB/c mice
215 were infected intraperitoneally with 1×10^8 PFU of HSV-1 suspended in 200 μL of 1×PBS.
216 After infection, mice were weighed daily to monitor disease progression and mice that
217 lost ≥30% of their initial body weight were deemed ethically dead. All mice were daily
218 monitored to the end of the experiment and biological death cause by vaccinia infection
219 were also recorded. For treatment experiments, mice were given equal moles of
220 candidate compounds dissolved in saline containing 5% DMSO, 10% Solutol, and 17%
221 SBE-β-CD via oral gavage at days 1, 3 and 5 post-infection as specified in Figure 4-6.
222 Control animals received an equivalent volume of the vehicle via the same gavage
223 method. Infected mice were euthanized at timepoints indicated in Figure 4-6. Samples
224 of multiple organs were collected for viral titration, host response assay or
225 pharmaceutical analysis.

226 **Pharmaceutical analyses of mouse tissue samples**

227 Anticoagulated mouse blood samples were collected and centrifuged at 3200 rpm for 10
228 minutes at 4°C to separate the plasma, which was then aliquoted and stored at -80°C
229 until analysis. Tissue samples, including spleen, brain, liver, kidney, lung, and testes,
230 were homogenized and centrifuged at 4100g for 15 minutes to obtain supernatants for

231 pharmacokinetic analysis. The concentrations of the candidate compounds,
232 intermediate metabolites, and active metabolites in both plasma and tissue samples
233 were determined using a validated liquid chromatography-tandem mass spectrometry
234 (LC-MS/MS) method, as described in the literature [38]. The lower limits of quantitation
235 (LLOQ) were 1 ng/mL in plasma, and in tissues, the LLOQs were 10 ng/g for ODE-(S)-
236 HPMPA and BCV, 20 ng/g for CDV, and 50 ng/g for HPMPA and HDP-(S)-HPMPA.

237 **Titration of Tiantan vaccinia and HSV-1 in mouse organs**

238 Tissue samples were pre-cooled on ice and homogenized using high-throughput tissue
239 grinding machine (Cat# Scientz-192, NingBo Scientz Biotechnology Co., Ningbo City,
240 China). After that, the homogenates were centrifuged at 2000g for 10 minutes and the
241 supernatants were collected for viral titration following similar procedures to those
242 described above for in vitro viral titration. Briefly, confluent monolayers of Vero cells in
243 24-well plates were inoculated with 10-fold serially diluted supernatants of tissue
244 homogenates. After incubation, the wells were overlaid with 800 μL of overlay medium
245 and incubated for 4 days. Finally, the plates were fixed with neutral formalin and stained
246 with crystal violet, and plaques were counted to determine viral titers.

247 **Histological examination**

248 Tissue samples of multiple mouse organs were collected at 7 days post Tiantan
249 vaccinia infection. Collected tissues were fixed in 4% neutral paraformaldehyde for 2
250 hours, followed by standard processing and embedding in paraffin. Tissue sections
251 were stained with hematoxylin and eosin (H&E). The stained slides were analyzed using
252 the KF-PRO-120 digital pathology slide scanner (KFBIO) to assess tissue morphology
253 and the extent of pathological changes. The images were analyzed and exported by K-
254 VIEWER1.5.5.6 software.

255 **Detection of cytokine transcription in mouse lung**

256 Total RNA was extracted from mouse lung tissues collected at multiple timepoints post
257 Tiantan vaccinia infection using Trizol reagent (Cat# 15596026CN, Life Technologies).
258 1 μg of total RNA from each sample was reversely transcribed using the HiScript II Q
259 RT SuperMix for qPCR (+gDNA wiper) (R223-01, Vazyme, China). Real-time PCR was
260 conducted with the TB Green® Premix Ex Taq™ II (Tli RNase H Plus) (Cat# RR820Q,
261 TaKaRa) using an ABI 7500 real-time fluorescence quantitative PCR (qPCR) instrument

262 (Thermo Fisher Technology Co., LTD., Shanghai, China). Transcription levels of
263 cytokine genes relative to the GAPDH gene were calculated using the $2^{-\Delta Ct}$ method,
264 where ΔCt = Ct of the target gene - Ct of GAPDH. The primers of mouse cytokines and
265 GAPDH genes used for qRT-PCR are listed in Supplemental table 1, which were
266 synthesized according to a previous work [39].

267 **Determination of Alanine Aminotransferase (ALT) in murine serum**

268 Peripheral blood was collected from mice at 2 days post the third dose of drug treatment.
269 Serum was separated after clotting at room temperature for 1 hour by centrifuging at
270 1000g for 10 minutes at 4°C. Serum ALT activity was determined using a
271 commercialized ELISA kit following the manufacturer's protocol (Cat# JL12668, Jianglai
272 Biotechnology, Shanghai, China). Optical density was measured at 450 nm using a
273 microplate reader (Cat# 800TS, Biotek, USA).

274 **Statistical methods**

275 Statistical analyses were conducted using GraphPad Prism 9 (GraphPad Software,
276 USA). The normality of the data was checked before all downstream statistical analyses.
277 Comparisons between two groups were performed by the method of t-test. Differences
278 among multiple groups were compared by the method of one-way ANOVA. EC_{50} and
279 EC_{90} values were calculated using a four-parameter variable slope non-linear
280 regression method. Survival curves were compared by the Cox-Mantel test. $P \leq 0.05$
281 was considered as statistically significant.

282

283 **Results**

284 **In vitro cytotoxicity and in vivo pharmacokinetics of candidate compounds**

285 Synthesized compounds (BCV formate, ODE-(S)-HPMPA formate and HDP-(S)-
286 HPMPA formate) were dissolved in DCM:MeOH (v:v=1:3) at a maximum concentration
287 of 10μM. Cytotoxicity assays showed that all compounds were well tolerated at
288 concentrations of 5μM and 10μM in Vero cells (Figure 2A and 2B).
289 To facilitate in vivo antiviral activity evaluation, we monitored the kinetics of absorption
290 and metabolism for each compound after a single dose of oral gavage in mice. Our data
291 showed that all compounds or their metabolites were detectable at a half hour post oral
292 administration (Figure 2C and 2D), suggesting that they could be quickly assimilated

293 into blood. After absorption, BCV formate, ODE-(S)-HPMPA formate and HDP-(S)-
294 HPMPA formate were instantly hydrolyzed into BCV, ODE-(S)-HPMPA and HDP-(S)-
295 HPMPA, respectively. And the concentrations of these metabolites in blood peaked
296 around 1 to 2 hours post oral administration (Figure 2C and 2D). Then, BCV was
297 gradually hydrolyzed into CDV within 24 hours post oral administration (Figure 2E).
298 While ODE-(S)-HPMPA and HDP-(S)-HPMPA were hydrolyzed faster into HPMPA,
299 which lasted only 8 hours (Figure 2F).

300 **ODE-(S)-HPMPA formate and HDP-(S)-HPMPA formate showed superior anti-**
301 **orthopoxvirus activities than BCV and BCV formate**

302 To compare the anti-orthopoxvirus effects of the candidate drugs with BCV, we firstly
303 tested their antiviral activities against vaccinia Tiantan strain and MPXV in vitro. Our
304 data showed that the EC_{50} and EC_{90} of BCV formate against Tiantan vaccinia were
305 similar with those of BCV, while the EC_{50} and EC_{90} of ODE-(S)-HPMPA formate and
306 HDP-(S)-HPMPA formate were conspicuously lower (Figure 3A). Notably, ODE-(S)-
307 HPMPA formate displayed the lowest EC_{50} and EC_{90}, which were around 15-fold lower
308 than BCV (Figure 3A). The anti-MPXV activity of BCV was similar with its effect against
309 Tiantan vaccinia, while the other three compounds inhibited MPXV even more potently
310 than Tiantan vaccinia (Figure 3B). ODE-(S)-HPMPA formate demonstrated the most
311 potent anti-MPXV effect, whose EC_{50} and EC_{90} were more than 40-fold lower than those
312 of BCV (Figure 3B).

313 Next, we evaluated the in vivo anti-orthopoxvirus activities of the synthesized
314 compounds using a lethal mouse model of vaccinia virus infection. As shown in Figure
315 4A, 4 weeks old BALB/c mice were intra nasally infected with 6×10^6 pfu of vaccinia
316 Tiantan strain. Equal moles of candidate drugs were given at 1 day, 3 days and 5 days
317 post infection via oral gavage. All groups of infected mice experienced obvious body
318 weight loss, which peaked around 7 to 8 days post infection for mice treated with BCV
319 formate, ODE-(S)-HPMPA formate or HDP-(S)-HPMPA formate (Figure 4B). In contrast,
320 mice received the vehicle or BCV underwent more severe weight loss and all mice in
321 these two groups ethically died by day 8 (Figure 4B). For animals in the group treated
322 with ODE-(S)-HPMPA formate, more than 90% of mice (10 out of 11) survived, a
323 significant improvement in the survival rate compared with animals in all other groups

324 (vehicle, BCV or BCV formate groups; Figure 4C). The second-best drug was HDP-(S)-
325 HPMPA formate, which protected significantly more mice from death than vehicle and
326 BCV (Figure 4C). BCV formate also displayed better protection, but its efficacy did not
327 significantly differ from those of the vehicle and BCV (Figure 4C).
328 To characterize the in vivo anti-vaccinia virus activities further, we repeated vaccinia
329 virus infection and drug treatment in mice, but this time 3-5 mice of each group were
330 euthanized at indicated time points for detections of viral replication, host responses
331 and drug metabolites (Figure 5A). We found that vaccinia virus resided mainly in lungs
332 after intra nasal infection and significant suppression of the virus by candidate drugs
333 could be observed in all detected tissues except kidney (Figure 5B-5G), where live
334 vaccinia viruses were rarely detected even in the non-treated group. Compared to BCV,
335 BCV formate, ODE-(S)-HPMPA formate and HDP-(S)-HPMPA formate tended to
336 decrease vaccinia virus titers in lungs, but statistical significance was only observed
337 between BCV and ODE-(S)-HPMPA formate at day 3 and between BCV and HDP-(S)-
338 HPMPA formate at day 5 (Figure 5B). Histopathology examination showed that ODE-
339 (S)-HPMPA formate and HDP-(S)-HPMPA formate diminished the size of lung lesions
340 caused by vaccinia infection compared to BCV and BCV formate at 7 days post
341 infection (Figure 5H). Meanwhile, no signs of infection-caused or drug-related pathology
342 were observed in other organs, including the kidney, spleen, testis, liver and brain
343 (Supplementary figure 1). We also monitored the cytokine responses in lungs at 3, 5, 7,
344 10 and 14 days post infection. We found that different drugs impacted lung inflammation
345 differentially (Supplementary figure 2). Of note, at 7 days post vaccinia infection
346 (approximately the nadir of mouse body weight change), the transcription levels of IL-6
347 in lungs of mice treated with ODE-(S)-HPMPA formate were significantly lower than
348 those of mice treated with vehicle or BCV (Supplementary figure 2A). While, the levels
349 of IL-12 and TNF-a transcripts in lungs of mice treated with ODE-(S)-HPMPA formate or
350 BCV formate were significantly higher than those of mice treated with vehicle or BCV
351 (Supplementary figure 2B and 2C). These findings were partially in accordance with a
352 previous study suggesting that HPMPA could activate TNF-a secretion [40].
353 We noticed that livers contained the highest concentrations of drug metabolites during
354 the whole process of drug treatments (Supplementary figure 3). Hence, we assessed

355 the liver toxicities of candidate drugs via measuring the serum ALT levels at day 7 (2
356 days post the third dose of drug treatment). The results showed that the average levels
357 of plasma ALT ranked as follows: HDP-(S)-HPMPA formate > BCV formate > BCV >
358 vehicle > ODE-(S)-HPMPA formate > uninfected control (Supplementary figure 4). Of
359 note, the ALT levels of BCV, BCV formate and HDP-(S)-HPMPA formate treated mice
360 were significantly higher than that in uninfected controls, while no significant difference
361 was observed among mice of ODE-(S)-HPMPA formate treated group, vehicle group,
362 and control group (Supplementary figure 4).

363 **ODE-(S)-HPMPA formate and HDP-(S)-HPMPA formate could suppress HSV-1**
364 **both in vivo and in vitro, but were less effective than BCV and BCV formate in**
365 **protecting mice against lethal infection**

366 As NAs usually have broad spectrum antiviral activity [41], we next compared the anti-
367 HSV-1 activities between the candidate drugs and BCV. The results of in vitro antiviral
368 assays indicated that the EC_{50} and EC_{90} of BCV formate and ODE-(S)-HPMPA formate
369 against HSV-1 were close to those of BCV, while the EC_{50} and EC_{90} of HDP-(S)-
370 HPMPA formate were slightly higher (Figure 6A). To validate this observation, we tested
371 their efficacies against HSV-1 lethal infection in vivo. As shown in Figure 6B, BALB/c
372 mice were intra peritoneally infected with 1×10^8 pfu of HSV-1 (strain-17) followed by the
373 same regimen of drug treatment with vaccinia infected mice. Our data showed that BCV
374 and BCV formate alleviated mouse body weight loss, whereas ODE-(S)-HPMPA
375 formate and HDP-(S)-HPMPA formate apparently did not (Figure 6C). Albeit ODE-(S)-
376 HPMPA formate and HDP-(S)-HPMPA formate provided significant protection against
377 lethal HSV-1 infection than the vehicle, their protection rates were significantly lower
378 than those of BCV and BCV formate (Figure 6D). It is intriguing to see that the adenine
379 analogs (ODE-(S)-HPMPA formate and HDP-(S)-HPMPA formate) were more effective
380 in protecting mice against vaccinia infection while less effective towards HSV-1 infection
381 compared to cytidine analogs (BCV and BCV formate). We further compared the
382 genomic DNA base composition of orthopoxvirus with that of HSV and found that
383 orthopoxviruses contain obviously less GC than HSV (Supplementary figure 5 and
384 Supplementary table 2). This difference might lead to that adenine analogs would have

385 more chance to be incorporated into orthopoxvirus genome, while the cytidine analogs
386 would be more frequently incorporated into HSV genome.
387 Inspired by this observation, we were curious whether a combined regimen of purine
388 and pyrimidine analogs would provide more balanced protection against orthopoxvirus
389 and herpesvirus. To test this hypothesis, we treated vaccinia infected mice with the
390 equal molar mixture of BCV formate and ODE-(S)-HPMPA formate, and treated HSV-1
391 infected mice with the equal molar mixture of BCV formate and ODE-(S)-HPMPA
392 formate (Supplementary figure 6A). The total dosage for each mixed regimen was
393 maintained in consistency with the aforementioned single-drug regimen. The result
394 showed that all mice survived after being treated with the combined regimens
395 (Supplementary figure 6B), which was obviously better than any single-drug treatment
396 (Figure 4 and Figure 6).
397 **Three candidate compounds exhibited better in vitro anti-hAdV activity than BCV**
398 BCV has been used compassionately to treat adenovirus infection for pediatric patients
399 receiving hematopoietic stem cell transplantation [42]. In this study, we compared the
400 anti-hAdV potencies between three candidate prodrugs and BCV using clinically
401 isolated strains of hAdV type C2 and type B21. Generally, the EC_{50} values of the three
402 candidates, especially those of BCV formate and ODE-(S)-HPMPA formate, were much
403 lower than the EC_{50} values BCV (Figure 7). Considering that the liver toxicity of ODE-
404 (S)-HPMPA formate were significantly lower than BCV formate (Supplementary figure 4),
405 we thought ODE-(S)-HPMPA formate could also be good candidate therapeutic for
406 hAdV infections.
407

408 **Discussion**

409 Nucleoside/nucleotide analogues (NAs) have been widely used to treat cancer and viral
410 diseases [43]. Given that the catalytic units of viral polymerases are conserved in their
411 structures [44], NAs are thought to be an important class of broad-spectrum antiviral
412 agents [41]. Since the first anti-viral NA was approved in 1969, more than two dozen
413 NAs have been licensed to treat viral infections [45]. However, only limited number of
414 viral diseases are targeted [3]. Among the six families of double stranded DNA viruses
415 (Hepadnaviridae, Polyomaviridae, Papillomaviridae, Adenoviridae, Herpesviridae

416 and Poxviridae) known to cause human diseases [46], only five viruses from three
417 families (Hepadnaviridae, Herpesviridae and Poxviridae) can be treated with approved
418 NAs [3, 4]. BCV is currently the only NA that can be used to treat human Mpox disease
419 under an FDA-authorized single-patient e-IND, while its efficacy is still inconclusive [47].
420 Bottlenecks, such as toxicity, poor oral bioavailability and limited translatability, restrain
421 NAs from being applied to more viral diseases [41, 45]. In this work, we and
422 collaborators synthesized a new precursor of CDV and two novel precursors of (S)-
423 HPMPA and evaluated their inhibitory activities against multiple double-stranded DNA
424 viruses, including orthopoxviruses, HSV-1 (strain 17) and human adenoviruses.
425 Through the experiments shown here, we found that BCV and three candidate prodrugs
426 exhibited varied antiviral potencies against different DNA viruses. The anti-
427 orthopoxvirus potency of BCV formate was non-inferior to BCV, by contrast the two
428 prodrugs of (S)-HPMPA were remarkably more effective than BCV in suppressing
429 orthopoxviruses both in vitro and in vivo. ODE-(S)-HPMPA formate was the best-
430 performing anti-orthopoxvirus compound, which displayed the most robust anti-
431 orthopoxvirus activity and the lowest hepatotoxicity. ODE-(S)-HPMPA formate and
432 HDP-(S)-HPMPA formate were designed based on previously reported ODE-(S)-
433 HPMPA and HDP-(S)-HPMPA [30, 33]. We did not test the latter compounds in parallel
434 in this study, but compared the data to that available in the literature [33], both ODE-(S)-
435 HPMPA formate and HDP-(S)-HPMPA formate are much more efficacious than their
436 counterparts in protecting mice from lethal vaccinia infection (Supplementary table 3).
437 The fact that ODE-(S)-HPMPA formate was more efficacious than HDP-(S)-HPMPA
438 formate in protecting mice against vaccinia infection might partly because ODE-(S)-
439 HPMPA formate distributed to lung more efficiently than HDP-(S)-HPMPA formate
440 (Supplementary figure 3).
441 A second key finding of this work is that BCV and BCV formate provided significantly
442 stronger protection against lethal HSV-1 infection than ODE-(S)-HPMPA formate and
443 HDP-(S)-HPMPA formate in mice. The primary anti-viral mechanism of NAs is that they
444 resemble natural nucleos(t)ides and act by being incorporated into the nascent DNA
445 chain [48, 49], however the mechanism underlying the varied protective effects against
446 orthopoxvirus and HSV-1 is not clear. As herpesvirus genome contains obviously more

447 GC than orthopoxvirus genome, we speculate that the cytidine analogs (BCV and BCV
448 formate) might be more effective in suppressing herpesviruses, while adenine analogs,
449 ODE-(S)-HPMPA formate and HDP-(S)-HPMPA formate, might inhibit orthopoxviruses
450 more efficiently. Consistent with this hypothesis, we proved that combined regimens of
451 cytidine and adenine analogs could provide excellent protection against both vaccinia
452 and HSV-1 infection in mice, indicating that combination of purine and pyrimidine
453 analogs might be a rational and promising strategy to develop a broad-spectrum
454 antiviral therapy.
455 Finally, we tested the anti-hAdV potencies of the candidate prodrugs through in vitro
456 experiments. Adenoviruses can cause life-threatening disease not only in
457 immunocompromised patients but also in the healthy, although the latter occurs less
458 frequently [50, 51]. Both CDV and BCV have been compassionately used to treat hAdV
459 infections in children receiving hematopoietic cell transplantation [42, 52], but there are
460 no officially approved therapeutics. Here we showed ODE-(S)-HPMPA formate could be
461 a good anti-hAdV agent, which exhibited a good safety profile and relatively stronger
462 inhibitory effect than BCV.
463 A major limitation of this work is that we did not test the in vivo anti-MPXV and anti-
464 hAdV effects of the candidate prodrugs, primarily because no appropriate animal
465 models are available to us. Evaluations using an MPXV infected rhesus macaque model
466 [53] and an hAdV infected human lung organoid model [54] may provide more relevant
467 data before moving any of the candidate prodrugs into clinical trials.
468

469 **Declaration of competing interests**

470 Patent applications regarding the novel prodrugs evaluated in this study have been
471 jointly filed by Shanghai Sci-Tech Inno Center for Infection & Immunity and Risen
472 (Shanghai) Pharma Tech Co., Ltd.. The authors declare no other competing interests.
473

474 **Author contributions**

475 Yanmin Wan, Wenhong Zhang and Youchun Wang jointly supervised the study. Yanmin
476 Wan, Zhaoqin Zhu and Chao Qiu designed the experiments. Yanmin Wan, Yifan Zhang,
477 Cuiyuan Guo, Jiasheng Lu, Yanan Zhou, Jiaojiao Zheng, Fahui Dai, Xiaoyang Cheng

and Kunlu Deng conducted the experiments. Yanmin Wan, Yifan Zhang and Cuiyuan Guo analyzed the data and drafted the manuscript. Yanmin Wan, Jiasheng Lu, Zhaoqin Zhu and Wanhai Wang revised the manuscript. All authors approved the submitted version.

Acknowledgments

We thank Quanlin Xue from Fudan University for kindly sharing HSV-1 (strain 17) with us. This work was supported in part by the National Natural Science Foundation of China (Grant No. 32270986), the major project of Study on Pathogenesis and Epidemic Prevention Technology System by the Ministry of Science and Technology of China (Grant No. 2021YFC2302500) and the National Key Research and Development Program of China (Grant No. 2022YFC2009802).

References

1. Lu, L., et al., *Antivirals with common targets against highly pathogenic viruses.* Cell, 2021. **184**(6): p. 1604-1620.
2. Peng, S., et al., *Progression of Antiviral Agents Targeting Viral Polymerases.* Molecules, 2022. **27**(21).
3. Palazzotti, D., et al., *Small Molecule Drugs Targeting Viral Polymerases.* Pharmaceuticals (Basel), 2024. **17**(5).
4. Chan-Tack, K., et al., *Benefit-risk assessment for brincidofovir for the treatment of smallpox: U.S. Food and Drug Administration's Evaluation.* Antiviral Res, 2021. **195**: p. 105182.
5. Magee, W.C. and D.H. Evans, *The antiviral activity and mechanism of action of (S)-[3-hydroxy-2-(phosphonomethoxy)propyl] (HPMP) nucleosides.* Antiviral Res, 2012. **96**(2): p. 169-80.
6. Bojkova, D., et al., *Drug Sensitivity of Currently Circulating Mpox Viruses.* N Engl J Med, 2023. **388**(3): p. 279-281.
7. Frenois-Veyrat, G., et al., *Tecovirimat is effective against human monkeypox virus in vitro at nanomolar concentrations.* Nat Microbiol, 2022. **7**(12): p. 1951-1955.
8. Byrareddy, S.N., et al., *Potential therapeutic targets for Mpox: the evidence to date.* Expert Opin Ther Targets, 2023. **27**(6): p. 419-431.
9. Duraffour, S., G. Andrei, and R. Snoeck, *Tecovirimat, a p37 envelope protein inhibitor for the treatment of smallpox infection.* IDrugs, 2010. **13**(3): p. 181-91.
10. Shamim, M.A., et al., *The use of antivirals in the treatment of human monkeypox outbreaks: a systematic review.* Int J Infect Dis, 2023. **127**: p. 150-161.
11. Adler, H., et al., *Clinical features and management of human monkeypox: a retrospective observational study in the UK.* Lancet Infect Dis, 2022. **22**(8): p. 1153-1162.
12. Barnes, A.H., et al., *Mpox: Special Considerations in the Immunocompromised Host.* Current Treatment Options in Infectious Diseases, 2022. **14**(4): p. 43-66.

13. Imran, M., et al., *Oral Brincidofovir Therapy for Monkeypox Outbreak: A Focused Review on the Therapeutic Potential, Clinical Studies, Patent Literature, and Prospects.* Biomedicines, 2023. **11**(2).
14. Grosenbach, D.W., et al., *Oral Tecovirimat for the Treatment of Smallpox.* N Engl J Med, 2018. **379**(1): p. 44-53.
15. Duraffour, S., et al., *ST-246 is a key antiviral to inhibit the viral F13L phospholipase, one of the essential proteins for orthopoxvirus wrapping.* J Antimicrob Chemother, 2015. **70**(5): p. 1367-80.
16. Smith, T.G., et al., *Tecovirimat Resistance in Mpox Patients, United States, 2022-2023.* Emerg Infect Dis, 2023. **29**(12): p. 2426-2432.
17. Alarcón, J., et al., *An Mpox-Related Death in the United States.* N Engl J Med, 2023. **388**(13): p. 1246-1247.
18. Lenharo, M., *Hopes dashed for drug aimed at monkeypox virus spreading in Africa.* Nature, 2024. **632**(8027): p. 965.
19. Andrei, G. and R. Snoeck, *Cidofovir Activity against Poxvirus Infections.* Viruses, 2010. **2**(12): p. 2803-30.
20. Lurain, N.S. and S. Chou, *Antiviral drug resistance of human cytomegalovirus.* Clin Microbiol Rev, 2010. **23**(4): p. 689-712.
21. Farlow, J., et al., *Comparative whole genome sequence analysis of wild-type and cidofovir-resistant monkeypoxvirus.* Virol J, 2010. **7**: p. 110.
22. Silva, N.I.O., et al., *Here, There, and Everywhere: The Wide Host Range and Geographic Distribution of Zoonotic Orthopoxviruses.* Viruses, 2020. **13**(1).
23. Zhang, Y., et al., *Potential threat of human pathogenic orthopoxviruses to public health and control strategies.* J Biosaf Biosecur, 2023. **5**(1): p. 1-7.
24. Shchelkunov, S.N., *An increasing danger of zoonotic orthopoxvirus infections.* PLoS Pathog, 2013. **9**(12): p. e1003756.
25. Shchelkunova, G.A. and S.N. Shchelkunov, *Smallpox, Monkeypox and Other Human Orthopoxvirus Infections.* Viruses, 2022. **15**(1).
26. De Clercq, E. and A. Holý, *Acyclic nucleoside phosphonates: a key class of antiviral drugs.* Nat Rev Drug Discov, 2005. **4**(11): p. 928-40.
27. Tollefson, A.E., et al., *Oral USC-093, a novel homoserinamide analogue of the tyrosinamide (S)-HPMPA prodrug USC-087 has decreased nephrotoxicity while maintaining antiviral efficacy against human adenovirus infection of Syrian hamsters.* Antiviral Res, 2024. **222**: p. 105799.
28. Luo, M., et al., *Amidate Prodrugs of Cyclic 9-(S)-[3-Hydroxy-2-(phosphonomethoxy)propyl]adenine with Potent Anti-Herpesvirus Activity.* ACS Med Chem Lett, 2018. **9**(4): p. 381-385.
29. Beadle, J.R., *Synthesis of cidofovir and (S)-HPMPA ether lipid prodrugs.* Curr Protoc Nucleic Acid Chem, 2007. **Chapter 15**: p. Unit 15.2.
30. Quenelle, D.C., et al., *Effect of oral treatment with (S)-HPMPA, HDP-(S)-HPMPA or ODE-(S)-HPMPA on replication of murine cytomegalovirus (MCMV) or human cytomegalovirus (HCMV) in animal models.* Antiviral Res, 2008. **79**(2): p. 133-5.
31. Dal Pozzo, F., et al., *In vitro evaluation of the anti-orf virus activity of alkoxyalkyl esters of CDV, cCDV and (S)-HPMPA.* Antiviral Res, 2007. **75**(1): p. 52-7.
32. Morrey, J.D., et al., *Alkoxyalkyl esters of 9-(s)-(3-hydroxy-2-phosphonomethoxypropyl) adenine are potent and selective inhibitors of hepatitis B virus (HBV) replication in vitro and in HBV transgenic mice in vivo.* Antimicrob Agents Chemother, 2009. **53**(7): p. 2865-70.

33. Quenelle, D.C., et al., *Effect of oral treatment with hexadecyloxypropyl-[(S)-9-(3-hydroxy-2- phosphonylmethoxypropyl)adenine] [(S)-HPMPA] or octadecyloxyethyl-(S)-HPMPA on cowpox or vaccinia virus infections in mice.* Antimicrob Agents Chemother, 2007. **51**(11): p. 3940-7.
34. Beadle, J.R., et al., *Synthesis and antiviral evaluation of alkoxyalkyl derivatives of 9-(S)-(3-hydroxy-2-phosphonomethoxypropyl)adenine against cytomegalovirus and orthopoxviruses.* J Med Chem, 2006. **49**(6): p. 2010-5.
35. Ruiz, J., et al., *Synthesis, metabolic stability and antiviral evaluation of various alkoxyalkyl esters of cidofovir and 9-(S)-[3-hydroxy-2-(phosphonomethoxy)propyl]adenine.* Bioorg Med Chem, 2011. **19**(9): p. 2950-8.
36. Grosche, L., et al., *Herpes Simplex Virus Type 1 Propagation, Titration and Single-step Growth Curves.* Bio Protoc, 2019. **9**(23): p. e3441.
37. Hartline, C.B., et al., *A standardized approach to the evaluation of antivirals against DNA viruses: Orthopox-, adeno-, and herpesviruses.* Antiviral Res, 2018. **159**: p. 104-112.
38. Painter, W., et al., *First pharmacokinetic and safety study in humans of the novel lipid antiviral conjugate CMX001, a broad-spectrum oral drug active against double-stranded DNA viruses.* Antimicrob Agents Chemother, 2012. **56**(5): p. 2726-34.
39. Wang, X., et al., *Immune Correlates of Disseminated BCG Infection in IL12RB1-Deficient Mice.* Vaccines (Basel), 2022. **10**(7).
40. Potmesil, P., et al., *Nucleotide analogues with immunobiological properties: 9-[2-Hydroxy-3-(phosphonomethoxy)propyl]-adenine (HPMPA), -2,6-diaminopurine (HPMPDAP), and their N6-substituted derivatives.* Eur J Pharmacol, 2006. **540**(1-3): p. 191-9.
41. Karim, M., C.W. Lo, and S. Einav, *Preparing for the next viral threat with broad-spectrum antivirals.* J Clin Invest, 2023. **133**(11).
42. Perruccio, K., et al., *Safety and efficacy of brincidofovir for Adenovirus infection in children receiving allogeneic stem cell transplantation: an AIEOP retrospective analyses.* Bone Marrow Transplant, 2021. **56**(12): p. 3104-3107.
43. Jordheim, L.P., et al., *Advances in the development of nucleoside and nucleotide analogues for cancer and viral diseases.* Nature Reviews Drug Discovery, 2013. **12**(6): p. 447-464.
44. Peersen, O.B., *A Comprehensive Superposition of Viral Polymerase Structures.* Viruses, 2019. **11**(8).
45. Jordheim, L.P., et al., *Advances in the development of nucleoside and nucleotide analogues for cancer and viral diseases.* Nat Rev Drug Discov, 2013. **12**(6): p. 447-64.
46. Modrow, S., et al., *Viruses with a Double-Stranded DNA Genome*, in *Molecular Virology*, S. Modrow, et al., Editors. 2013, Springer Berlin Heidelberg: Berlin, Heidelberg. p. 625-873.
47. Li, P., et al., *Clinical Features, Antiviral Treatment, and Patient Outcomes: A Systematic Review and Comparative Analysis of the Previous and the 2022 Mpox Outbreaks.* J Infect Dis, 2023. **228**(4): p. 391-401.
48. *Nucleoside Analogues*, in *LiverTox: Clinical and Research Information on Drug-Induced Liver Injury*. 2012, National Institute of Diabetes and Digestive and Kidney Diseases: Bethesda (MD).
49. Kamzeeva, P.N., et al., *Recent Advances in Molecular Mechanisms of Nucleoside Antivirals.* Curr Issues Mol Biol, 2023. **45**(8): p. 6851-6879.
50. Khanal, S., P. Ghimire, and A.S. Dhamoon, *The Repertoire of Adenovirus in Human Disease: The Innocuous to the Deadly.* Biomedicines, 2018. **6**(1).

614 51. Dotan, M., et al., *Adenovirus can be a serious, life-threatening disease, even in*
615 *previously healthy children.* Acta Paediatr, 2022. **111**(3): p. 614-619.
616 52. Hiwarkar, P., et al., *Brincidofovir is highly efficacious in controlling adenoviremia in*
617 *pediatric recipients of hematopoietic cell transplant.* Blood, 2017. **129**(14): p. 2033-2037.
618 53. Aid, M., et al., *Mpox infection protects against re-challenge in rhesus macaques.* Cell,
619 2023. **186**(21): p. 4652-4661.e13.
620 54. Zhao, S., et al., *Generation of Human Embryonic Stem Cell-Derived Lung Organoids for*
621 *Modeling Infection and Replication Differences between Human Adenovirus Types 3*
622 *and 55 and Evaluating Potential Antiviral Drugs.* J Virol, 2023. **97**(5): p. e0020923.

623

624 **Figure Legends**

625 **Figure 1 Illustration of the molecular formulae and the theoretical metabolic**
626 **pathways of BCV and the newly synthesized prodrugs**

627 After two steps of hydrolysis, BCV formate can be converted to the same active parent
628 drug (CDV) with BCV. ODE-(S)-HPMPA formate and HDP-(S)-HPMPA formate also
629 take two steps of hydrolysis to turn into HPMPA.

630

631 **Figure 2 In vitro cytotoxicity and in vivo pharmacokinetic analyses of BCV and**
632 **the candidate compounds**

633 (**A-B**) Comparisons of cytotoxicities between candidate compounds and BCV. Limited
634 by the solubility of BCV formate, ODE-(S)-HPMPA formate and HDP-(S)-HPMPA
635 formate, the highest concentration employed in the cytotoxicity assay was 10μM. All
636 compounds were tested in quadruplicated wells and the solvent was used as the
637 negative control to calculate the percentage of cell viabilities. Data are presented as
638 mean ± SD. (**C-D**) Plasma concentrations of BCV, BCV formate, ODE-(S)-HPMPA
639 formate and HDP-(S)-HPMPA formate, as well as their respective one-step hydrolytic
640 metabolites CDV, BCV, ODE-(S)-HPMPA and HDP-(S)-HPMPA, were measured at
641 various time points following a single oral gavage dose (3 mice per group). (**E-F**)
642 Plasma concentrations of BCV, ODE-(S)-HPMPA, and HDP-(S)-HPMPA, as well as
643 their hydrolytic metabolites (CDV and HPMPA) were measured at various time points
644 following a single oral gavage dose (3 mice per group).

645

646 **Figure 3 In vitro evaluations of anti-vaccinia and anti-MPXV activities of BCV and**
647 **the candidate compounds**

648 Vero cells were infected with vaccinia Tiantan strain (**A**) or MPXV (**B**) and treated with
649 the indicated concentrations of BCV or the candidate prodrugs. All compounds were
650 tested in triplicated wells at each concentration. The solvent was used as the non-
651 treated control. The antiviral effects were determined by calculating the reduction in
652 plaque formation. Data are presented as mean ± SD.

653

654 **Figure 4 ODE-(S)-HPMPA formate and HDP-(S)-HPMPA formate showed superior**
655 **therapeutic efficacies against lethal Tiantan vaccinia infection in mice**
656 (**A**) The schematic illustration of experimental design. (**B-C**) Weight loss and survival
657 rates of mice after being intra nasally infected with the vaccinia Tiantan strain. Mice
658 received the solvent served as the non-treated control. Weight loss ≥30% of initial body
659 weight was recorded as ethical death and was therefore not represented in the figure.
660 The data of weight loss are presented as mean ± SD. Mice that lost ≥30% of their initial
661 body weight were deemed ethically dead. Statistical significance is indicated as follows:
662 *, $, #: $p < 0.05$; **, $$, ##: $p < 0.01$; ***, $$$, ###: $p < 0.001$; ****, $$$$, ####: $p <$
663 0.0001.
664
665 **Figure 5 ODE-(S)-HPMPA formate and HDP-(S)-HPMPA formate more effectively**
666 **reduced lung vaccinia virus titers and mitigated pathological severity compared**
667 **to BCV and BCV formate**
668 (**A**) The schematic illustration of experimental design. (**B-G**) Viral titers in the lung,
669 spleen, kidney, brain, testis, and liver were measured by plaque assays at 3, 5, 7, 10,
670 and 14 days post-infection, respectively. (**H**) Histopathological examination of lung
671 tissue at 7 days post infection. Black outlines indicate areas of observed pathology, and
672 the percentages of the lesion area relative to the total area of the tissue are denoted in
673 red.
674
675 **Figure 6 Evaluations of in vivo and in vitro anti-HSV-1 potencies of BCV and the**
676 **candidate prodrugs**
677 (**A**) Vero cells were infected with HSV-1 stain 17 and treated with indicated
678 concentrations of BCV or the candidate compounds. All compounds were tested in
679 triplicated wells at each concentration. The solvent was used as the non-treated control.
680 The antiviral effects were determined by calculating the reduction in plaque formation.
681 Data are presented as mean ± SD. (**B**) The schematic illustration of in vivo experiment
682 design. (**C-D**) Weight loss and survival rates of mice after being intra
683 peritoneally infected with HSV-1. Mice received the solvent served as the non-treated
684 control. The data of weight loss are presented as mean ± SD. Weight loss ≥30% of initial

685 body weight was recorded as ethical death and was therefore not represented in the
686 figure. Statistical significance is indicated as follows: *, $, #: $p < 0.05$; **, $$, ##: $p <$
687 0.01; ***, $$$, ###: $p < 0.001$; ****, $$$$, ####: $p < 0.0001$.
688
689 **Figure 7 In vitro evaluation of anti-hAdV activities of BCV and the candidate**
690 **compounds**
691 Vero cells were infected with either hAdV C2 (**A**) or hAdV B21 (**B**) and subsequently
692 treated with indicated concentrations of BCV or the candidate prodrugs. All compounds
693 were tested in quadruplicate at each concentration. The solvent was used as the non-
694 treated control. Data are presented as mean ± SD.
695
696
697
698
699
700
701
702
703
704

705 **Supplementary figure legends**

706 **Supplementary figure 1 No signs of infection-caused or drug-related pathology**
707 **were detected in key organs post Tiantan vaccinia infection**

708 Histopathological examination of the kidneys, spleen, testis, liver, and brain in mice at 7
709 days post Tiantan vaccinia infection.

710

711 **Supplementary figure 2 Drug treatment impacted pulmonary cytokine responses**
712 **in mice following intranasal infection with Tiantan vaccinia**

713 The transcriptional levels of IL-6 (**A**), IL-12 (**B**), TNF-α (**C**), IL-2 (**D**), IL-1β (**E**), IFN-γ (**F**),
714 IL-4 (**G**) in lung tissues were assessed at 3, 5, 7, 10, and 14 days post-infection with the
715 Tiantan vaccinia virus.

716

717 **Supplementary figure 3 Monitoring in vivo drug metabolites throughout the**
718 **treatment course**

719 (**A-D**) The concentrations of drug metabolites in mouse plasma, lung, kidney, spleen
720 and liver were measured using HPLC-MS at 3, 5, 7, 10 and 14 days post infection,
721 respectively (3 mice per group). Metabolites of all drugs were non-detectable in the
722 brain and testis at any time point. Data are presented as mean ± SD.

723

724 **Supplementary figure 4 Detection of ALT levels in mouse serum**

725 Serum ALT levels were measured at 2 days after the third dose drug treatment (n=5).
726 Data are presented as mean ± SD.

727

728 **Supplementary figure 5 Comparison of genome GC content between Tiantan**
729 **vaccinia and HSV-1**

730 A representative Tiantan vaccinia genome sequence (accession number: KC207811.1)
731 and a representative HSV-1 genome sequence (accession number: X14112.1) were
732 retrieved from GenBank. The GC content was analyzed using a sliding window
733 approach in the Biostrings package of R package, with a window size of 1000 base
734 pairs.

735

736 **Supplementary figure 6 Adenine and cytidine analog combinations showed**
737 **complete protection against both vaccinia and HSV-1 infections**
738 (**A**) The schematic illustration of experimental design. (**B**) Weight loss of mice after
739 being infected with Tiantan vaccinia or HSV-1. Data are presented as mean ± SD.

Figure 1

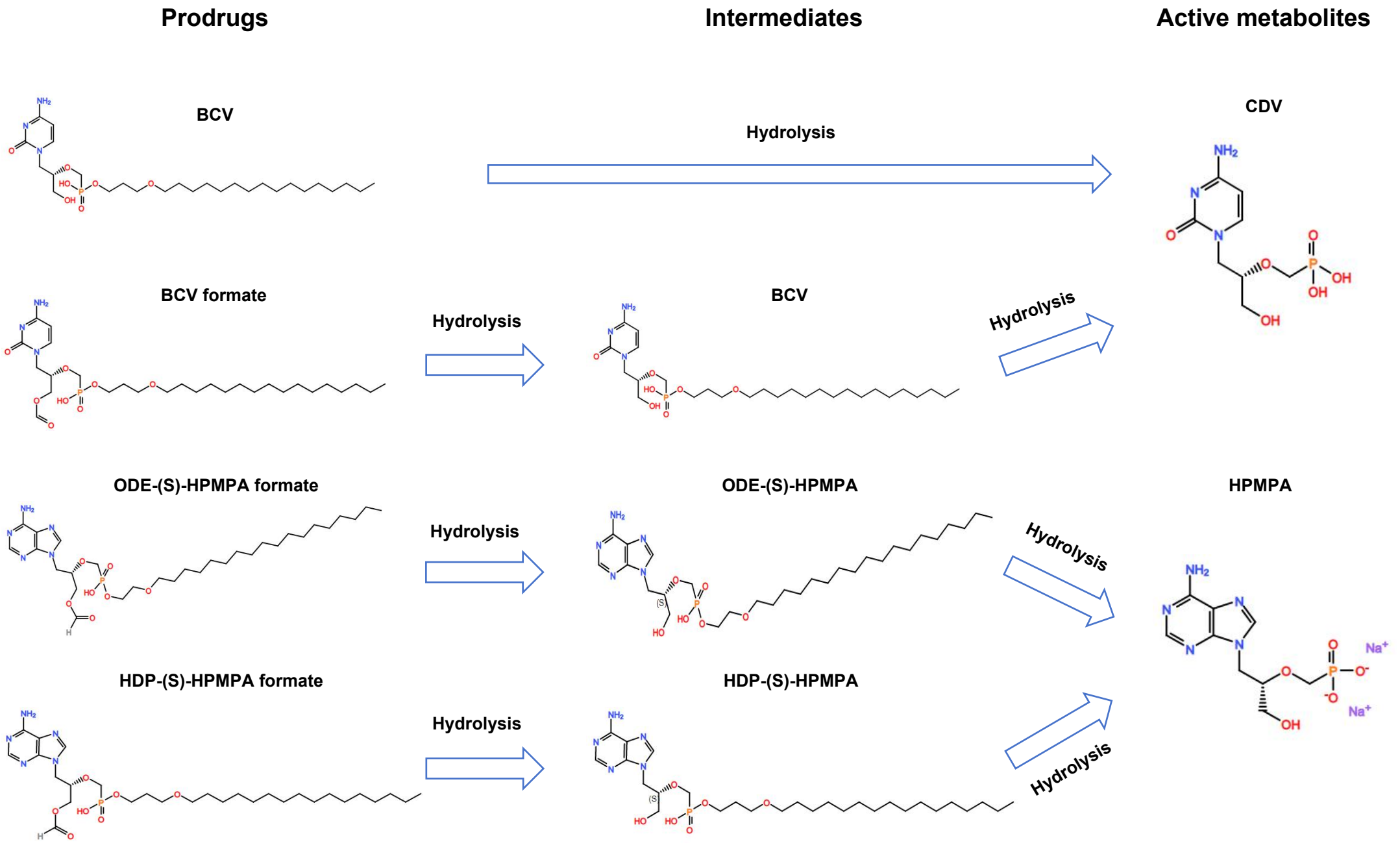
Prodrugs
Intermediates
Active metabolites
BCV
Hydrolysis
CDV
BCV formate
Hydrolysis
BCV
Hydrolysis
ODE-(S)-HPMPA formate
Hydrolysis
ODE-(S)-HPMPA
Hydrolysis
HPMPA
HDP-(S)-HPMPA formate
Hydrolysis
HDP-(S)-HPMPA
Hydrolysis

Figure 2

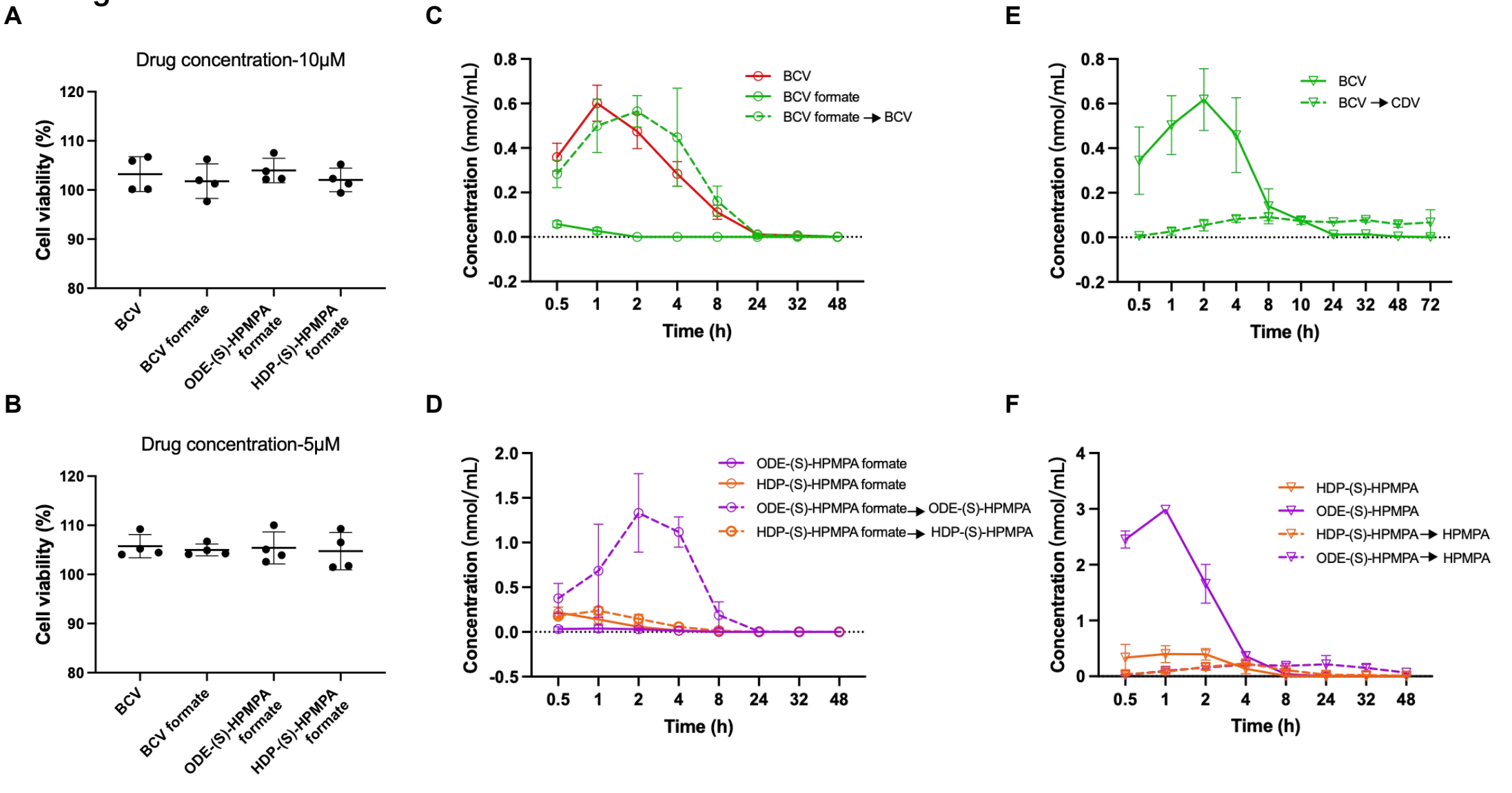
A
Drug concentration-10μM
Cell viability (%)
120
110
100
90
80
BCV
BCV formate
ODE-(S)-HPMPA formate
HDP-(S)-HPMPA formate
B
Drug concentration-5μM
Cell viability (%)
120
110
100
90
80
BCV
BCV formate
ODE-(S)-HPMPA formate
HDP-(S)-HPMPA formate
C
Concentration (nmol/mL)
0.8
0.6
0.4
0.2
0.0
-0.2
0.5
1
2
4
8
24
32
48
Time (h)
BCV
BCV formate
BCV formate → BCV
D
Concentration (nmol/mL)
2.0
1.5
1.0
0.5
0.0
-0.5
0.5
1
2
4
8
24
32
48
Time (h)
ODE-(S)-HPMPA formate
HDP-(S)-HPMPA formate
ODE-(S)-HPMPA formate → ODE-(S)-HPMPA
HDP-(S)-HPMPA formate → HDP-(S)-HPMPA
E
Concentration (nmol/mL)
0.8
0.6
0.4
0.2
0.0
-0.2
0.5
1
2
4
8
10
24
32
48
72
Time (h)
BCV
BCV → CDV
F
Concentration (nmol/mL)
4
3
2
1
0
0.5
1
2
4
8
24
32
48
Time (h)
HDP-(S)-HPMPA
ODE-(S)-HPMPA
HDP-(S)-HPMPA → HPMPA
ODE-(S)-HPMPA → HPMPA

Figure 3

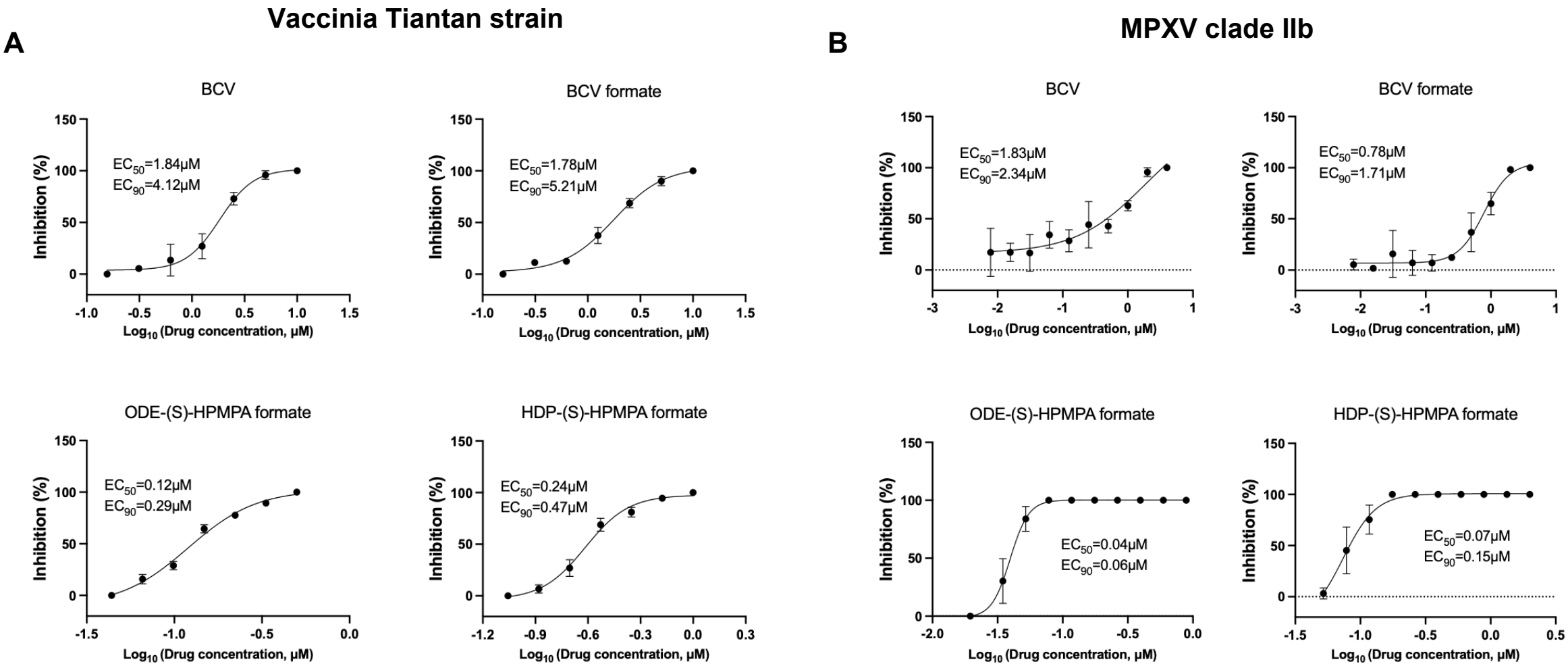
A
Vaccinia Tiantan strain
BCV
EC50=1.84μM
EC90=4.12μM
BCV formate
EC50=1.78μM
EC90=5.21μM
ODE-(S)-HPMPA formate
EC50=0.12μM
EC90=0.29μM
HDP-(S)-HPMPA formate
EC50=0.24μM
EC90=0.47μM
B
MPXV clade IIb
BCV
EC50=1.83μM
EC90=2.34μM
BCV formate
EC50=0.78μM
EC90=1.71μM
ODE-(S)-HPMPA formate
EC50=0.04μM
EC90=0.06μM
HDP-(S)-HPMPA formate
EC50=0.07μM
EC90=0.15μM
Inhibition (%)
Log10 (Drug concentration, μM)

Figure 4

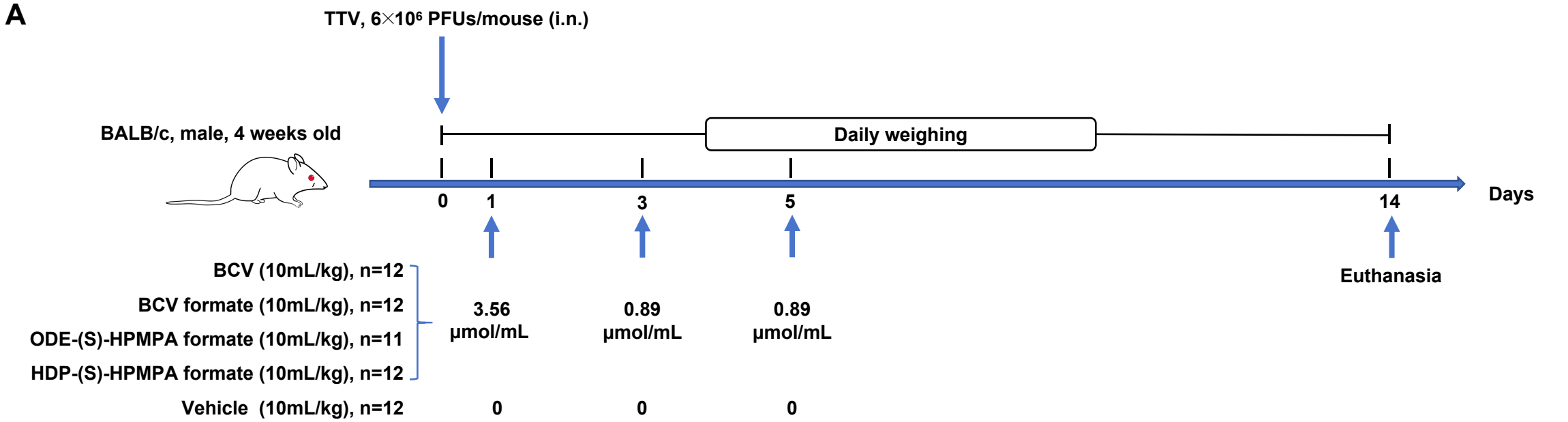
A
TTV, 6×10⁶ PFUs/mouse (i.n.)
BALB/c, male, 4 weeks old
Daily weighing
0
1
3
5
14
Days
Euthanasia
BCV (10mL/kg), n=12
BCV formate (10mL/kg), n=12
ODE-(S)-HPMPA formate (10mL/kg), n=11
HDP-(S)-HPMPA formate (10mL/kg), n=12
3.56 μmol/mL
0.89 μmol/mL
0.89 μmol/mL
Vehicle (10mL/kg), n=12
0
0
0

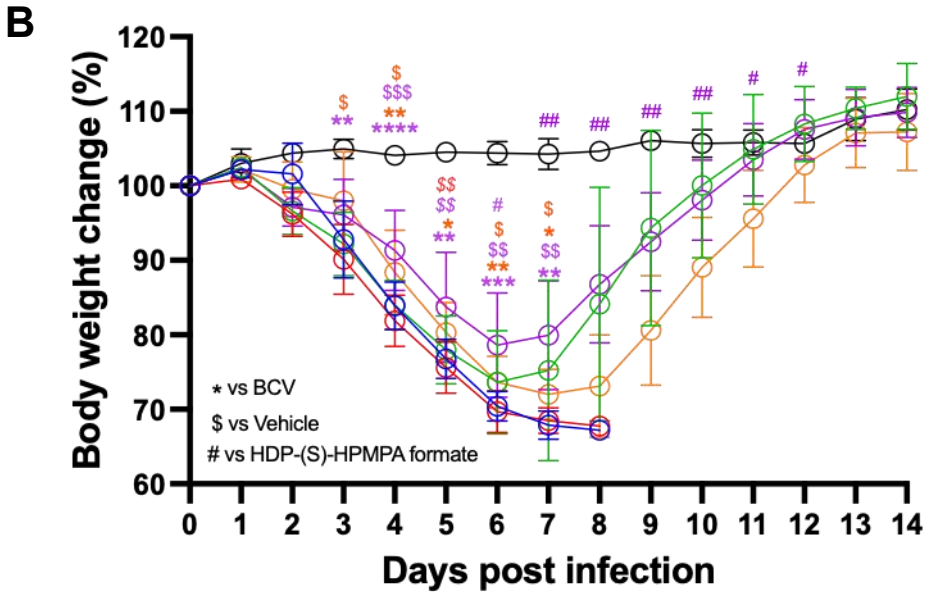
B
Body weight change (%)
Days post infection
* vs BCV
$ vs Vehicle
# vs HDP-(S)-HPMPA formate

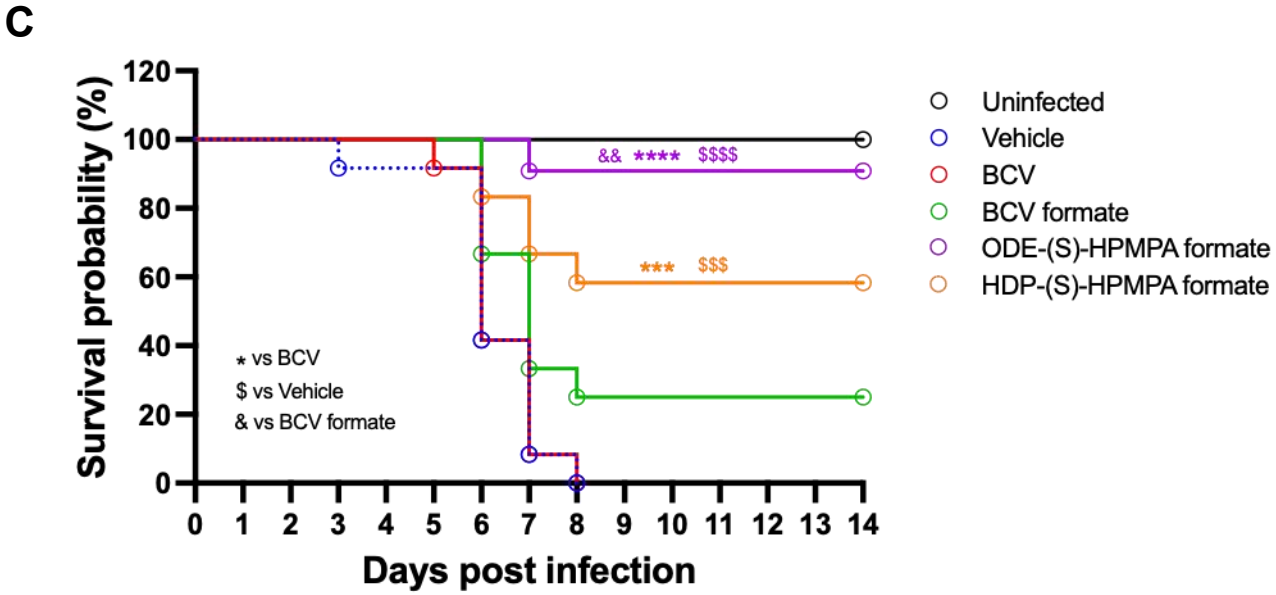
C
Survival probability (%)
Days post infection
* vs BCV
$ vs Vehicle
& vs BCV formate
Uninfected
Vehicle
BCV
BCV formate
ODE-(S)-HPMPA formate
HDP-(S)-HPMPA formate

Figure 5

A

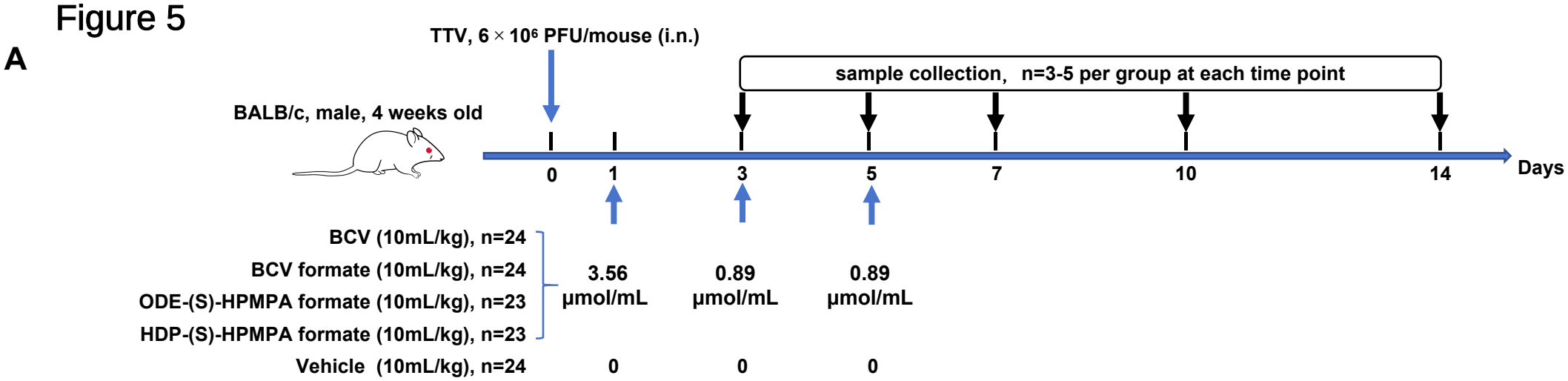
TTV, 6 × 10⁶ PFU/mouse (i.n.)
sample collection, n=3-5 per group at each time point
BALB/c, male, 4 weeks old
0
1
3
5
7
10
14
Days
BCV (10mL/kg), n=24
BCV formate (10mL/kg), n=24
ODE-(S)-HPMPA formate (10mL/kg), n=23
HDP-(S)-HPMPA formate (10mL/kg), n=23
3.56 μmol/mL
0.89 μmol/mL
0.89 μmol/mL
Vehicle (10mL/kg), n=24
0
0
0

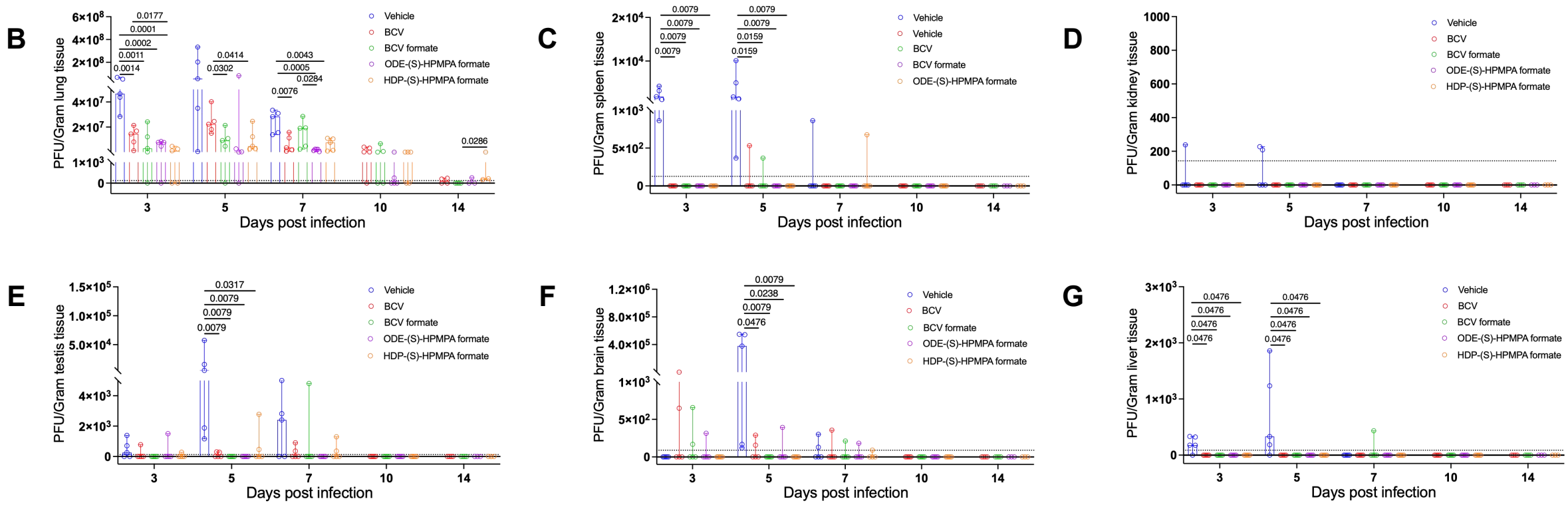
B
PFU/Gram lung tissue
C
PFU/Gram spleen tissue
D
PFU/Gram kidney tissue
E
PFU/Gram testis tissue
F
PFU/Gram brain tissue
G
PFU/Gram liver tissue
Vehicle
BCV
BCV formate
ODE-(S)-HPMPA formate
HDP-(S)-HPMPA formate
Days post infection

H

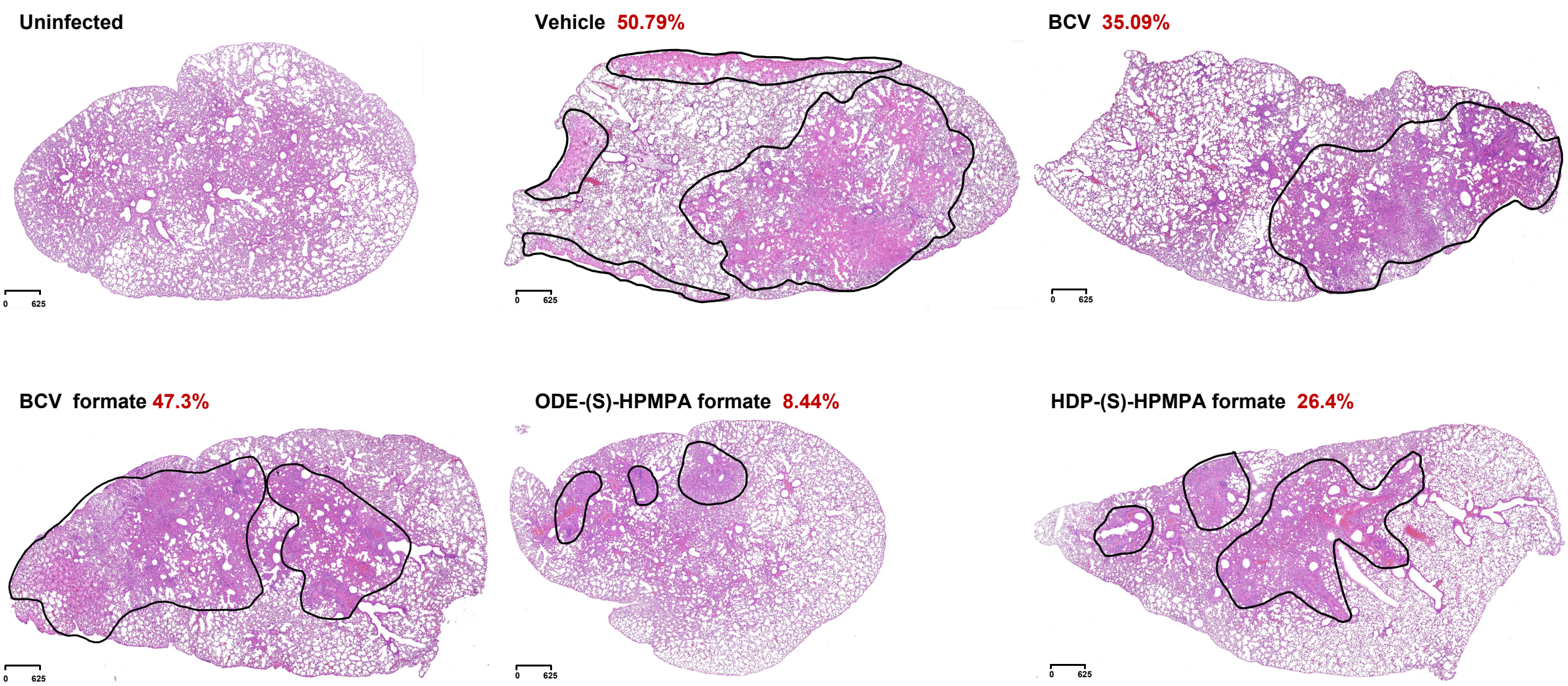
Uninfected
Vehicle 50.79%
BCV 35.09%
BCV formate 47.3%
ODE-(S)-HPMPA formate 8.44%
HDP-(S)-HPMPA formate 26.4%
0
625

Figure 6

A

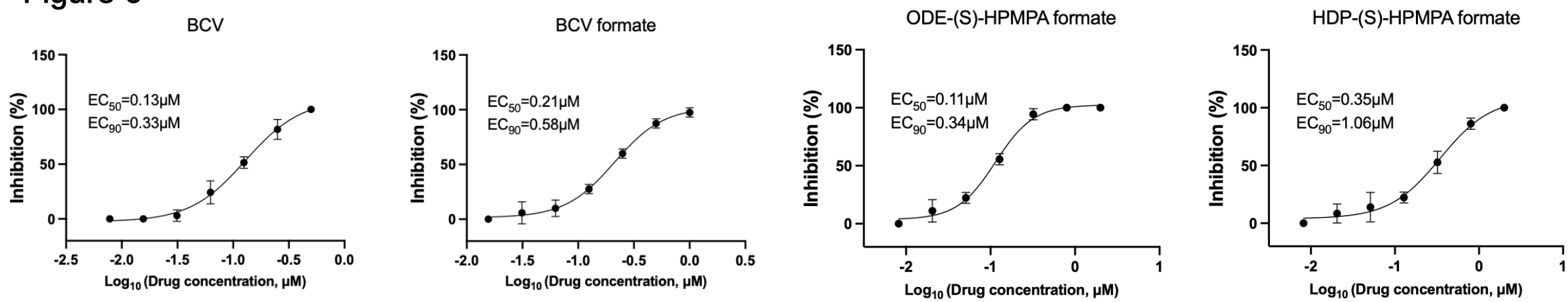

B

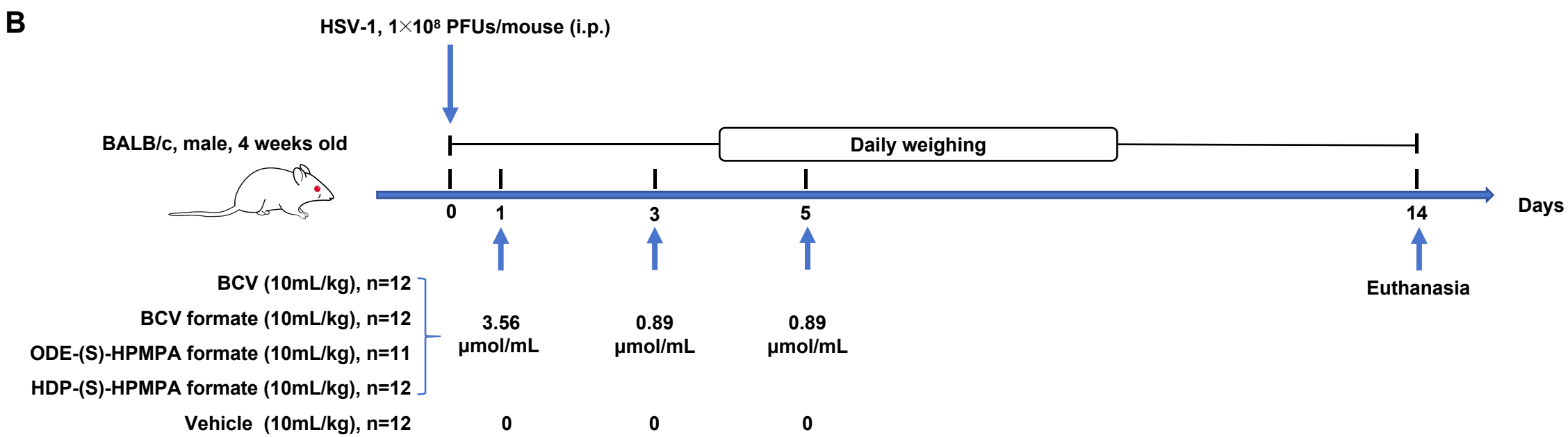

C

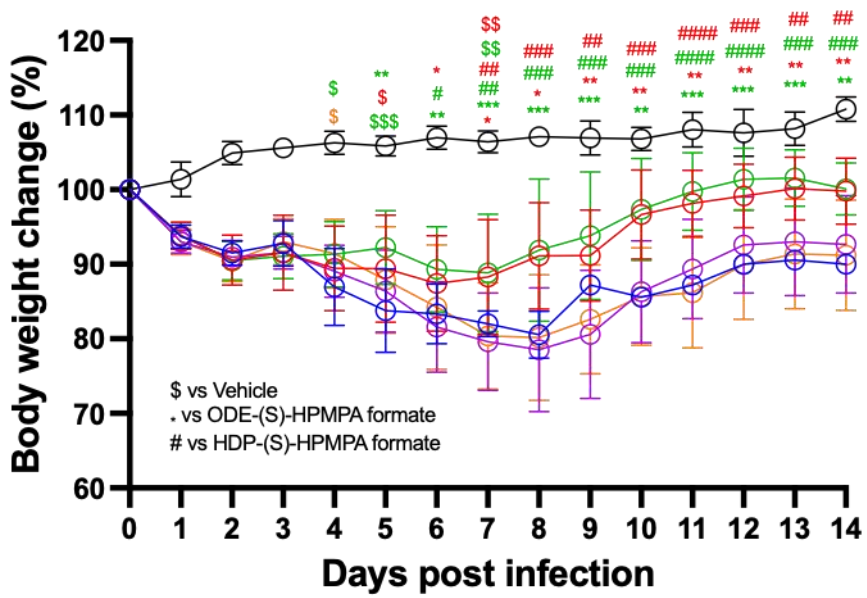

D

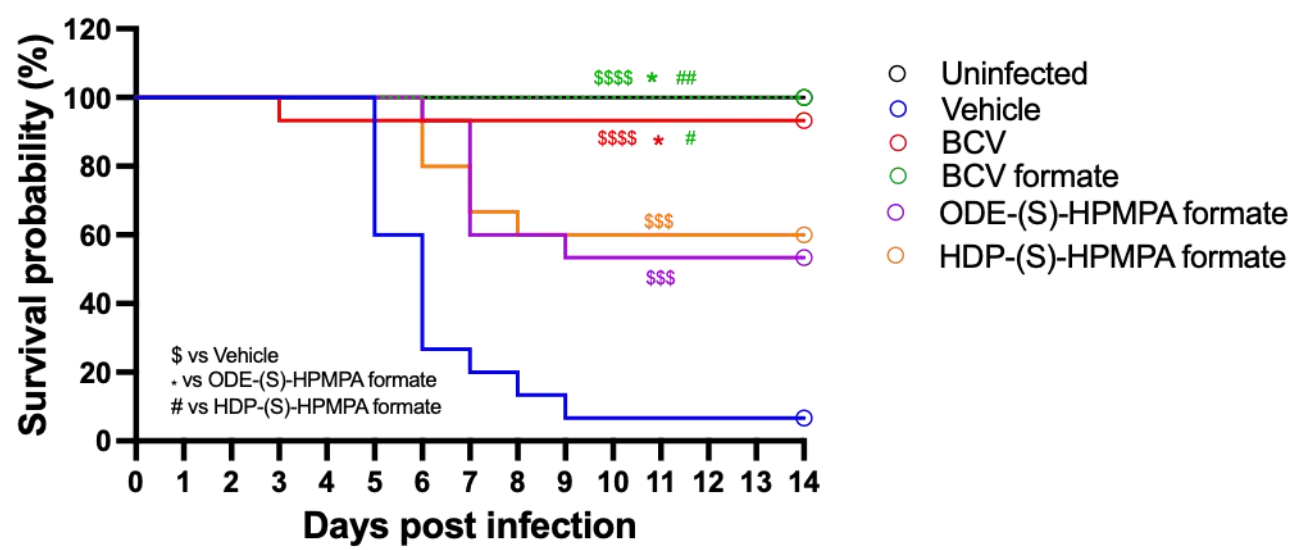

Figure 7

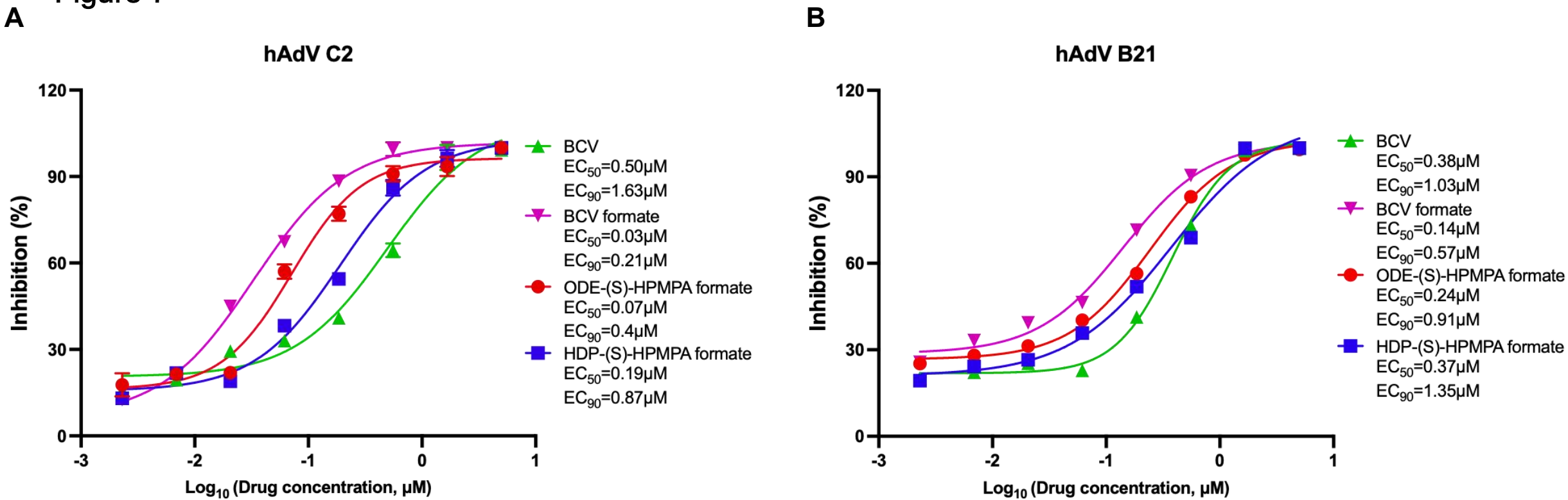
A
hAdV C2
Inhibition (%)
120
90
60
30
0
-3
-2
-1
0
1
Log10 (Drug concentration, μM)
BCV
EC50=0.50μM
EC90=1.63μM
BCV formate
EC50=0.03μM
EC90=0.21μM
ODE-(S)-HPMPA formate
EC50=0.07μM
EC90=0.4μM
HDP-(S)-HPMPA formate
EC50=0.19μM
EC90=0.87μM
B
hAdV B21
Inhibition (%)
120
90
60
30
0
-3
-2
-1
0
1
Log10 (Drug concentration, μM)
BCV
EC50=0.38μM
EC90=1.03μM
BCV formate
EC50=0.14μM
EC90=0.57μM
ODE-(S)-HPMPA formate
EC50=0.24μM
EC90=0.91μM
HDP-(S)-HPMPA formate
EC50=0.37μM
EC90=1.35μM

Supplementary figure 1

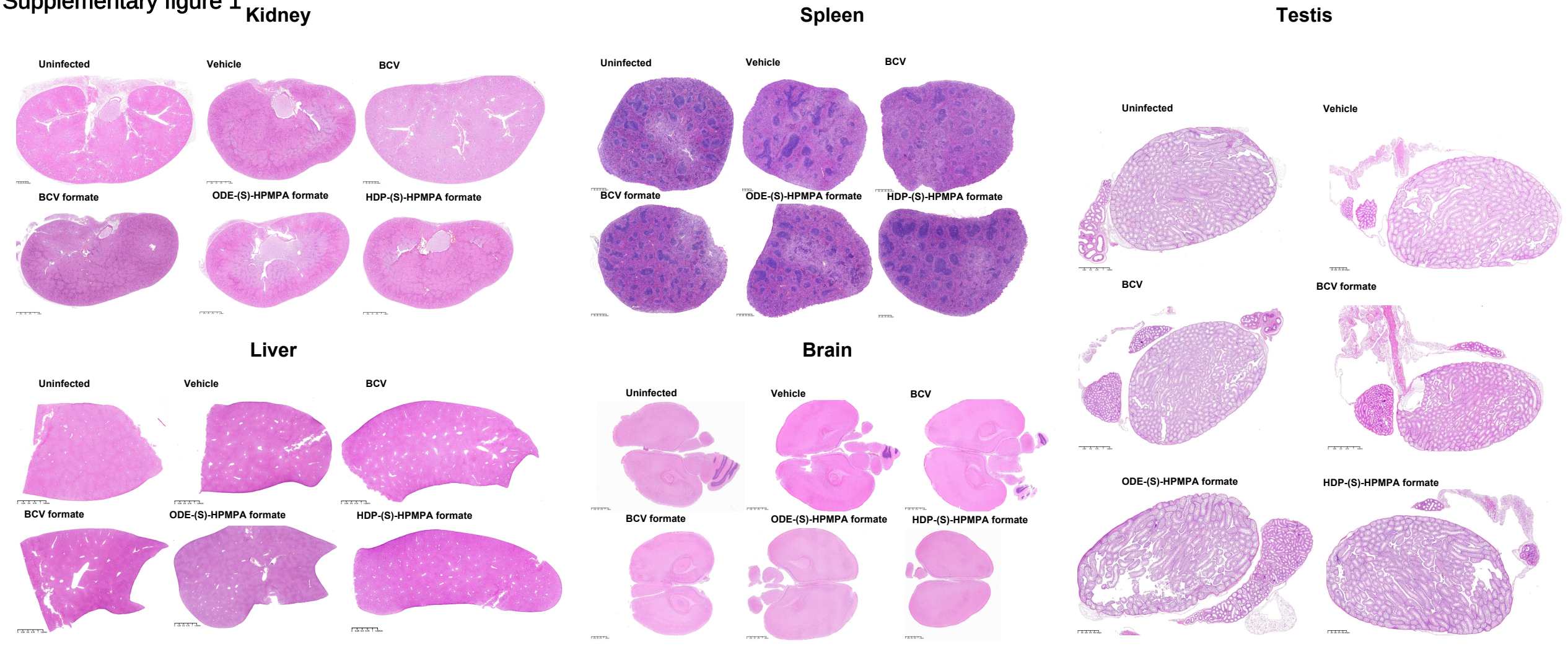

Supplementary figure 2

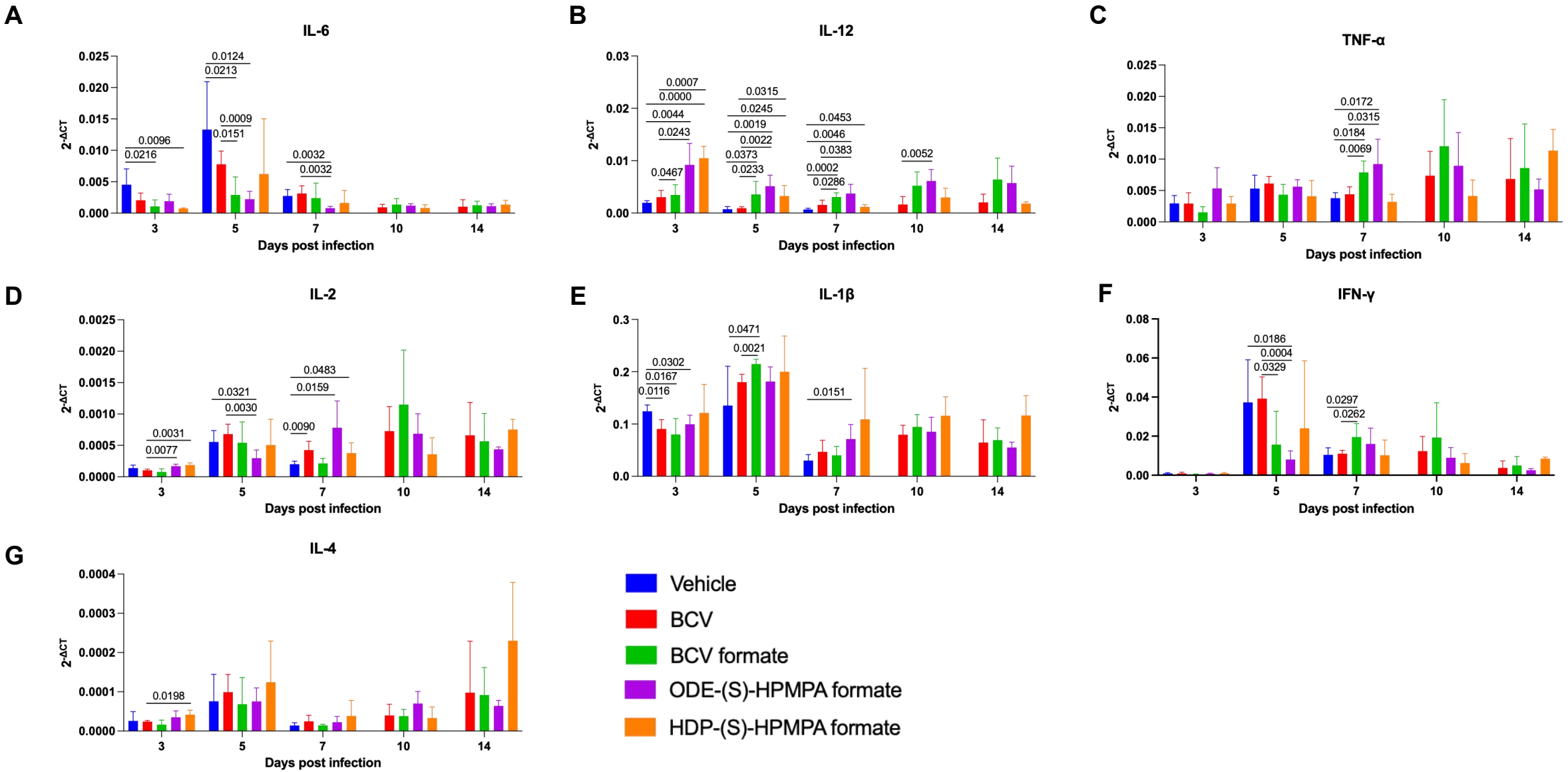

Supplementary figure 3

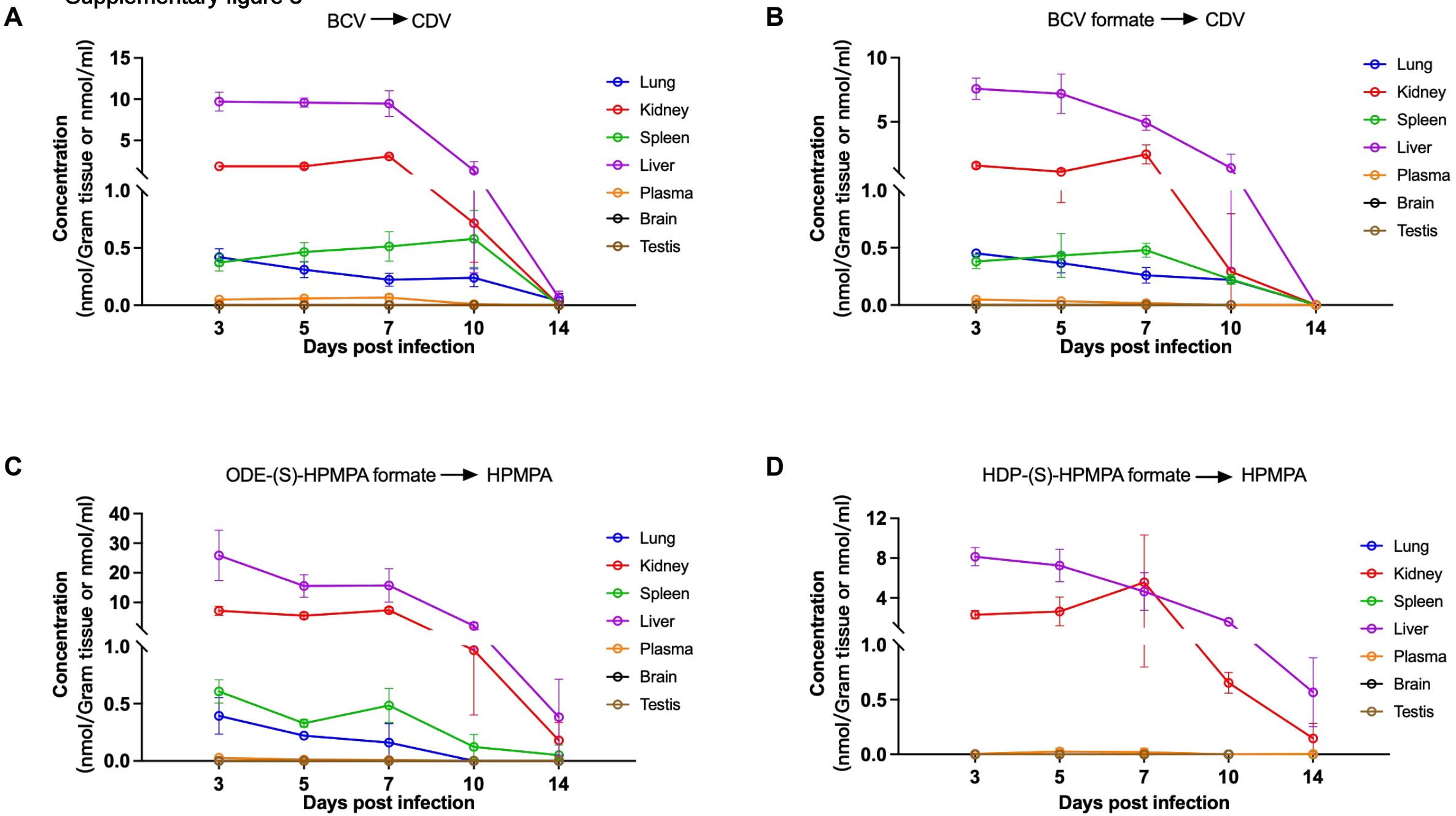

Supplementary figure 4

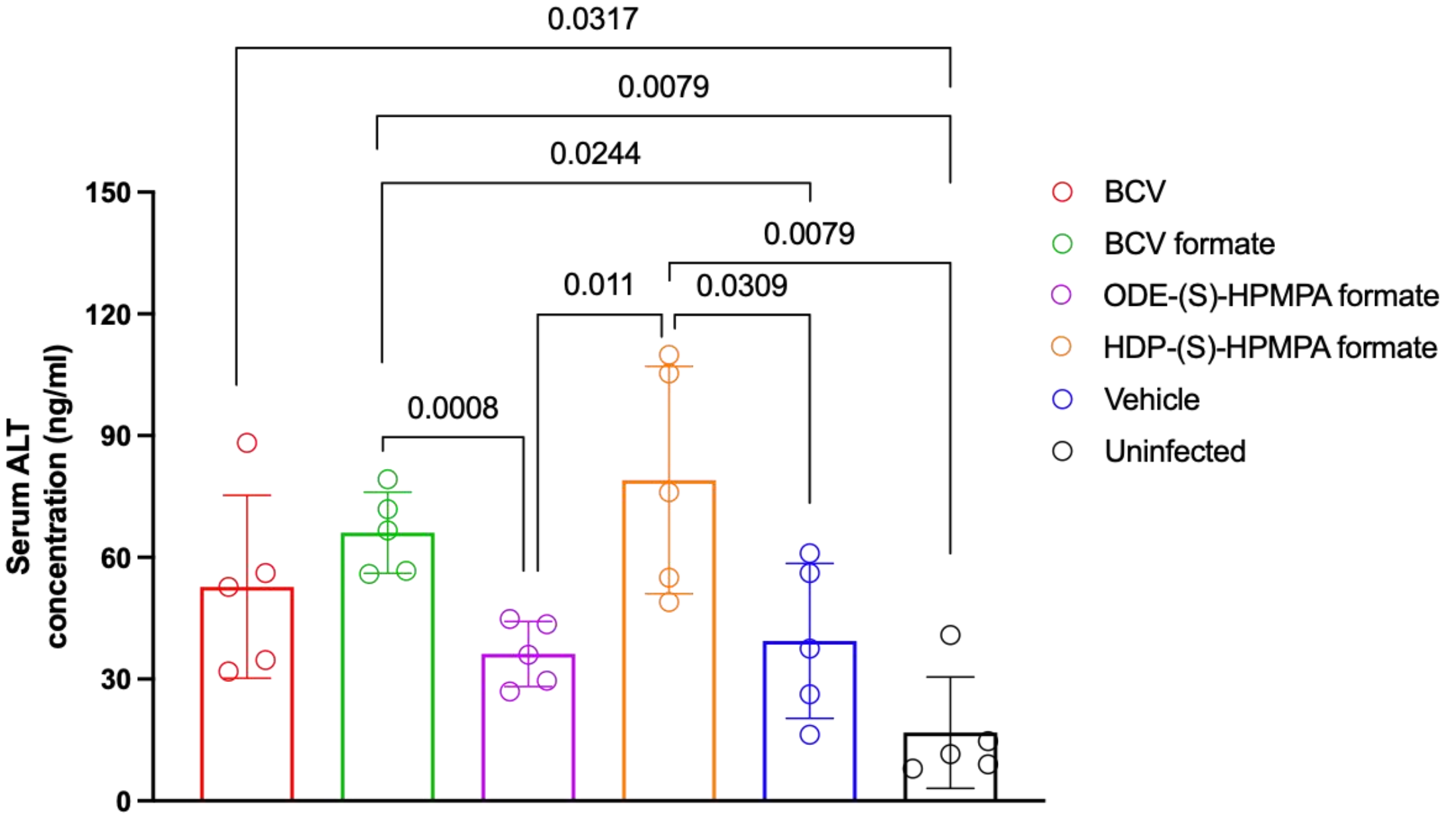

Supplementary figure 5

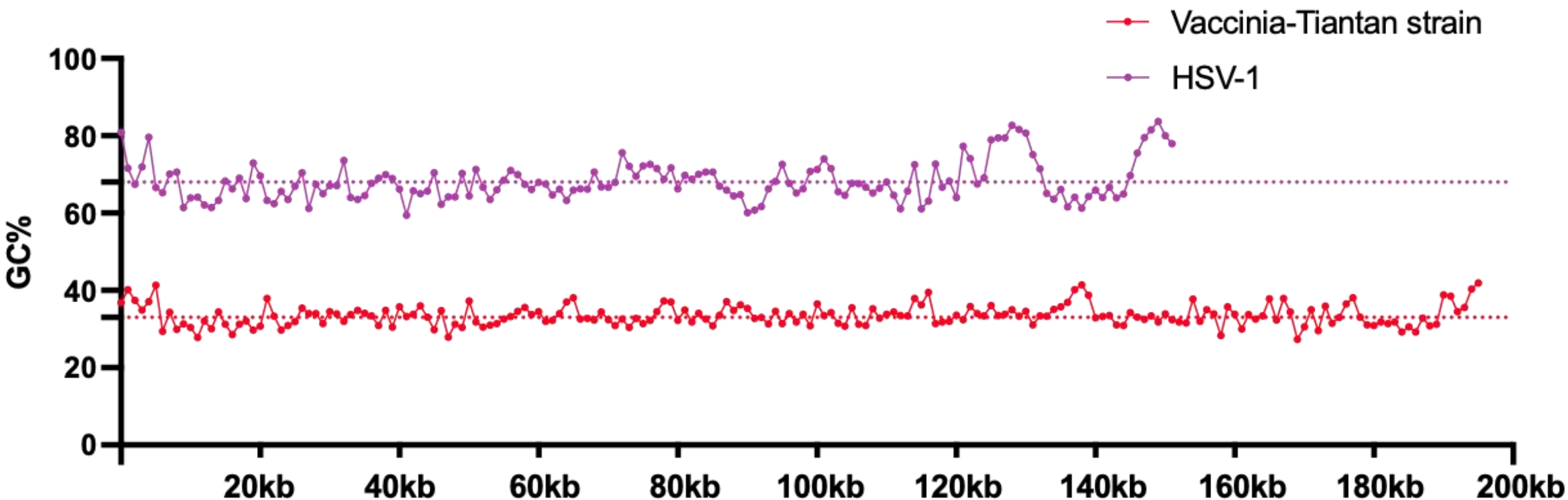

Supplementary figure 6

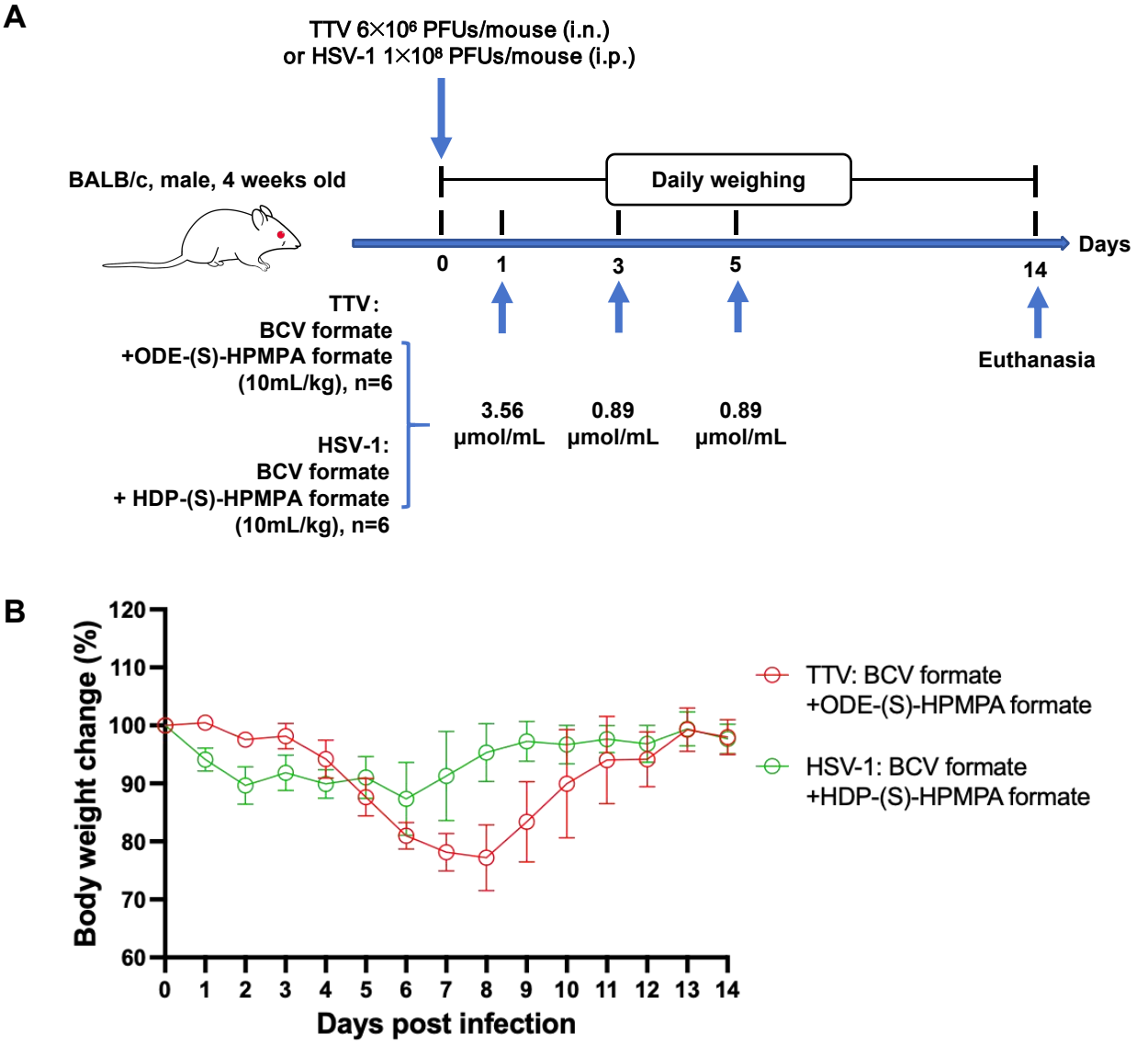

Supplementary table 1 Primer sequences used for quantitative PCR assays of murine cytokines

Gene		Primer sequence 5' to 3'
GAPDH	FP	ACCCAGAAGACTGTGGATGG
	RP	GGATGCAGGGATGATGTTCT
IL6	FP	GAGGATACCACTCCCAACAGACC
	RP	AAGTGCATCATCGTTGTTCATACA
IL-1β	FP	CAACCAACAAGTGATATTCTCCATG
	RP	GATCCACACTCTCCAGCTGCA
TNF-α	FP	CATCTTCTCAAAATTCGAGTGACAA
	RP	TGGGAGTAGACAAGGTACAACCC
IL-2	FP	TCTGCGGCATGTTCTGGATTT
	RP	ATGTGTTGTCAGAGCCCTTTAG
IFN-γ	FP	ACAGCAAGGCGAAAAAGGATG
	RP	TGGTGGACCACTCGGATGA
IL-4	FP	ATCGGCATTTTGAACGAGGTC
	RP	GAGGACGTTTGGCACATCCA
IL-12	FP	CTGTGCCTTGGTAGCATCTATG
	RP	CGCAGAGTCTCGCCATTATGAT
IL-10	FP	AAGCCTTATCGGAAATGATCCA
	RP	GCTCCACTGCCTTGCTCTTATT

FP: Forward primer; RP: Reverse primer

Supplementary table 2 GC content analyses of representative genomes of orthopoxviruses and herpesviruses

Virus	GenBank Number	GC%
Vaccinia virus strain TianTan	KC207811.1	33
Vaccinia virus WR	AY243312.1	33
Monkeypox virus clade IIb B.1	ON676708.1	33
Monkeypox virus clade Ib	PP601207.1	33
Monkeypox virus clade Ia	PP601206.1	33
Cowpox virus	NC_003663.2	33
Variola virus	PP405600.1	33
Human herpesvirus 1	X14112.1	68
Human herpesvirus 2	NC_001798.2	70
Human cytomegalovirus	X17403.1	57
Epstein-Barr virus	V01555.2	60

Supplementary table 3 Both ODE-(S)-HPMPA formate and HDP-(S)-HPMPA formate are more efficacious than ODE-(S)-HPMPA and HDP-(S)-HPMPA in protecting mice from lethal vaccinia infection

Compound	Treatment schedule and dosage	Ratio of biological death	Observation period
ODE-(S)-HPMPA formate	Oral gavage at day 1 (22.4 mg/kg), days 3 and 5 (5.59 mg/kg) after infection with Tiantan vaccinia [$]	0/11	14 days
HDP-(S)-HPMPA formate	Oral gavage at day 1 (21.9 mg/kg), days 3 and 5 (5.46 mg/kg) after infection with Tiantan vaccinia [$]	0/12	
ODE-(S)-HPMPA [£]	Oral gavage once daily at 30 mg/kg for 5 days starting 1 day after infection with vaccinia WR strain	2/15	21 days
HDP-(S)-HPMPA [£]		2/15	

[$] The mass dose was calculated to ensure the molar doses of the two drugs were equal.

[£] Values were reported previously [33].